Critical analysis of thermal conductivity enhancement of alumina–water nanofluids

M. Iqbal[1] · K. Kouloulias[1] · A. Sergis[1] · Y. Hardalupas[1]

Abstract

Nanofluids are colloidal suspensions constituted of nanoparticles and typical heat transfer fluids which have shown potential in yielding enhanced heat transport for many applications. Significant attention has been paid to their thermal conductivity enhancement which has been alleged, in some cases, to exceed theoretical limits classifying the enhancement as "anomalous". The present study aims to quantitatively investigate the nature of the enhancements reported in the literature and classify their alignment with theoretical predictions. To do so, a rigorous and objective mathematical analysis method has been employed. The novelty and value of the present work lies in the deeper characterisation and understanding of the anomalous observations reported. The present analytical study focuses on (spherical) Al_2O_3–water nanofluids. It was discovered that studies involving low nanoparticle concentrations ($\phi \leq 0.2$ vol%) and the use of electrostatic stabilisation (through pH control) as opposed to steric stabilisation (using surfactants) as suspension stability control methods are likely to report anomalous effects. An exceptional case was observed for $d < 15$ nm, where to achieve anomalous enhancement, surfactants and pH controllers should not be used to prevent significant interfacial resistance. The shared characteristics of these anomalous observations indicate that nanofluid preparation effects are linked to the underlying physical mechanisms of heat transfer involved and those should be further investigated. The failure of studies attempting to replicate anomalous thermal conductivity enhancement in the literature could hence be understood, as these did not satisfy the conditions required to lead to an anomalous enhancement. The role of measurement errors was also considered.

Abbreviations

EMT	Effective medium theory
HS	Hashin–Shtrikman
IEP	Isoelectric point
MDS	Molecular dynamics simulations
MZI	Mach–Zehnder interferometry
SEM	Scanning electron microscopy
TEM	Transmission electron microscopy
THW	Transient hot wire
THWe	Transient hot wire (electrically conductive sensor)
TPS	Transient plane source
VdW	Van der Waals

Greek symbols

β	Ratio of effective nanoparticle thermal conductivity to individual nanoparticle thermal conductivity (–)
μ	Dynamic viscosity (Pa s)
ν	Kinematic viscosity ($m^2\ s^{-1}$)
τ	Particle relaxation time (s)
ϕ	Nanoparticle volumetric percentage (v/v%) (–)
ρ	Density (kg m^{-3})

List of symbols

c_p	Specific heat capacity($J\ kg^{-1}\ K^{-1}$)
d	Nanoparticle nominal (manufacturer stated) diameter (nm)
k	Thermal conductivity (W $m^{-1}\ K^{-1}$)
k_B	Boltzmann constant (J K^{-1})
N	Number of publications (–)
n	Number of observations (–)
n'	Number of observations per publication (–)
Pr	Prandtl number (–)
R^2	Regression coefficient (–)

✉ M. Iqbal
  mi4517@ic.ac.uk

[1] Department of Mechanical Engineering, Imperial College London, South Kensington SW7 2AZ, UK

r	Nanoparticle radius (nm)
r_c	Nanoparticle cluster/agglomerate radius (nm)
S	Standard error of regression (–)
Re	Reynolds number (–)
T	Temperature (K)
V	Nanoparticle volumetric fraction (v/v) (–)
X	Nanoparticle mass fraction (m/m) (–)

Subscripts

bf	Basefluid
l	Nano-layer
min	Minimum
nf	Nanofluid
p	Particle
r	Reduced dataset
sample	Sample

Introduction

Nanofluids are colloidal solutions of a base fluid within which nanoparticles (with diameters $d < 100$ nm) are suspended with concentrations below 1 vol%. They have received significant attention from the scientific community due to their potential for enhancing heat transfer; however, their underlying physical mechanisms are yet to be fully understood. In the literature, both enhancement and deterioration have been observed, depending on the characteristics of the nanofluid, the heat transfer mode, the operating conditions and the apparatus considered. Many of these parameters either were not fixed or remained unreported (for example, time between nanofluid preparation and measurement, particle size distribution in suspension). This has created substantial 'noise' in the reported results which, unavoidably, make the field difficult to navigate. Most importantly, the complexity of quantifying the unknown boundary conditions and resulting nanofluid thermal performance has hindered their commercial deployment.

Regarding recent works on anomalous thermal conductivity enhancement in nanofluids, Hashimoto et al. [1] reported anomalous enhancement in an SiO_2 nanofluid (up to 11% enhancement in thermal conductivity, exceeding theoretical predictions). This result is highly interesting, as SiO_2 has a lower thermal conductivity compared to metal oxides such as Al_2O_3, yet still provides significant thermal enhancement. This led the authors to hypothesise that the enhancement is arising not from the contribution of the higher thermal conductivity of the dispersed phase, but by some effect of the dispersed phase on the bulk phase. To investigate this, they conducted neutron and X-ray scattering in addition to Raman spectroscopy to investigate the interactions of the bulk fluid molecules and the dispersed phase. They found the adsorbed liquid layer to be less than 10 nm, and the dispersed phase

to cause significant effects on the vibrational states of the fluid molecules. In essence, the dispersed phase was found to be acting as an impediment, reducing the mean free path of the fluid molecules and enhancing phonon conduction in the liquid, enhancing the thermal conductivity.

Hashimoto et al. [2] also reported anomalous enhancement for the same nanofluid in a forced convection system (for the same pumping loss, an 18% enhancement was reported with 300 nm diameter particles). They also observed particle size to affect the thermal conductivity and convective heat transfer enhancement. Somarathna et al. [3] demonstrated that anomalous thermal conductivity enhancement reported in molecular dynamics simulation (MDS) studies can be attributed to the application of the Green–Kubo method, which is insufficient to fully define the system. Instead, using a non-equilibrium MD approach, more sensible results are obtained. For their Argon-Copper system ($\phi = 4.5$ vol%), they found interfacial effects to dominate and suppress other mechanisms such as micro-convection. This latter result is expected, as they used incredibly small particle sizes (diameters from 1 to 10 nm). Interestingly, they observed the arrangement of chain-like structures to yield up to a 67% enhancement in the thermal conductivity, without incurring a viscosity increment, strengthening the case for this augmenting mechanism.

Woo et al. [4] used a high-power laser to ablate a graphite target in deionised water, reporting up to 82% enhancement in thermal conductivity for the smallest particle size and highest concentration obtained ($d = 109.5$ nm, 0.062 mass%). The nanofluids field has developed further, with the introduction of magnetic nanofluids, otherwise known as 'ferrofluids'. Vinod and Phillip [5] detailed recent advances in these fluids, which exhibit good thermal conductivity enhancement without viscosity increment under conditions of small, monodisperse particle size distributions—advantageous for pumping applications. The application of a magnetic field to these fluids is seen to enhance the thermal conductivity due to the formation of chain-like structures up to a critical field strength, after which the enhancement reduces to a reduction in the aspect ratio of the agglomerates. In addition to offering tuneable thermal performance, these effects demonstrate the importance of particle size distribution and the arrangement of the dispersed phase in determining thermal performance.

The thermal performance of nanofluids under the four major modes of heat transport (conduction, convection, pool boiling and flow boiling) has been widely investigated and reviewed in the literature [6–11]—with lack of agreement even between similar reported boundary conditions. To evaluate the discrepancy between reported results, Sergis and Hardalupas [9] conducted a statistical analysis of published nanofluid thermal performance data in an attempt to evaluate the trends of 'noisy' datasets. This study reported the most

common thermal performance and associated deviations for a given system and summarised the proposed physical mechanisms responsible for the identified trends.

Although useful in clearly elucidating what performance to expect—on average—for a given system condition, no significant progress has been made towards a feasible, testable theory on the fundamental thermal performance on nanofluids. Recommendations have been made in the literature to improve standardisation, encouraging researchers to provide a standard set of parameters associated with their work. These include but are not limited to:

- pH (or zeta potential)
- Surfactant type and concentration (if used)
- Concentration

  o Ideally in volumetric percentage, as volume effects dominate at the small length scales present in nanofluid systems

- Ultrasonication time, power, device type

  o Lower power, ultrasonic baths are preferred over high power, ultrasonic probes [12]

- TEM analysis (shape, particle size distribution)

  o Many studies do not present TEM images, which means there is no verification of the nano-powder properties reported by the manufacturer
  o We have previously reported on discrepancies between manufacturer-stated and observed properties in a nano-powder product sourced from a reputable supplier. The nanoparticles were claimed to be spherical and of a certain size, however from TEM analysis the particles were in fact seen to be non-uniform in size and shape (non-spherical) [13]

- Time between ultrasonication and experiment

  o Nanofluid stability is the dominant parameter that determines nanofluid thermal performance
  o Even small differences in time between the completion of ultrasonic dispersion and experimentation (on the order of hours) can have significant effects on stability—which will reduce over time—and hence thermal performance

By standardising the data, the effects of individual parameters that we are interested in can be isolated and understood clearly, without discrepancy. The above is one of the key reasons current replication studies in the literature have not succeeded [14]. The above protocol should be tested and iterated upon, to ensure that independent system variables that contribute significantly to the measured outcome remain fixed. For example, it may be that there is a tolerance for allowing some flexibility in the time between ultrasonication and experimentation without significantly affecting the reported results.

Given that the landscape of nanofluid research and applications has not significantly progressed due to a lack of repeatability and a continued discrepancy in the reported data, additional research into these issues and what can be done to resolve them is needed. The previous study by Sergis and Hardalupas [9] did not consider parameters linked to stability (pH and surfactant use), and the parametric analysis was limited due to the small sample sizes for each heat transfer mode given the wide scope of the study. Hence to extend the application and statistical power of the trend analyses, system parameters such as nanoparticle material must be fixed. Thus, the scope of the present critical analysis was reduced to experimental thermal conductivity performance of alumina–water nanofluids. Thermal conductivity was chosen as it is the most fundamental heat transfer mode, and without an adequate understanding at this level it is not sensible to introduce higher-mode phenomena. Alumina–water was chosen as the nanofluid at is the most widely studied, enabling the collation of a large dataset.

Quantifying the effects of variations in nanofluid stability (as inferred by reported pH, zeta potential or surfactant usage) on thermal performance, combined with the data on nanoparticle concentration and size, led to novel insights that have not been previously reported in the literature to our knowledge. These insights explained a lot of the discrepancy of the literature, especially in studies that attempted to replicate 'anomalous' thermal conductivity enhancement. This study presents, and reports on the boundary condition-dependent nature of anomalous thermal conductivity enhancement in alumina nanofluids, although in theory this behaviour should extend to other materials.

With such a vast dataset, the accuracy of theoretical and semi-empirical models of nanofluid thermal conductivity presented in the literature could also be assessed. Several models exist, building upon classical Maxwellian theory [15] by attempting to account for the additional postulated mechanisms of heat transport, such as Brownian motion induced nanoconvection. From our data, nanofluids exhibit two distinct modes of thermal conductivity enhancement, and by segregating the data based on these modes, the resulting accuracy of the models was improved. Nanofluids that exhibit anomalous enhancement have a distinct behaviour from those that exhibit conventional enhancement, and so they must be modelled differently. Our approach to this issue is detailed in this paper, with the most accurate models for each enhancement mode providing some indication of the responsible underlying physical mechanisms.

The main aim of the present study is to critically assess reported observations of anomalous thermal conductivity

enhancement in alumina–water nanofluids reported in the literature. As part of this assessment, the number of independent researchers observing the anomaly is identified which allowed a deeper investigation into the experimental conditions observed (e.g. nanoparticle concentration and stabilisation methods employed). Correlation of specific experimental conditions leading to the anomalies could hence be identified and examined further in order to offer additional understanding on the underlying mechanisms causing them.

The paper is structured as follows. First, the methodology of the present critical analysis is presented. This covers the scope of the study in terms of the considered nanofluid, how publications were sourced and what types of publications were considered, how the database was formulated and processed to minimise bias, how the considered thermal conductivity models were selected and how their accuracy was quantified.

From this basis, we generate a set of results, which is presented in the following section. The probability distribution of the reported enhancement in thermal conductivity for alumina–water nanofluids is presented to gauge the typical thermal performance to expect for this nanofluid, in addition to allowing the quality of the sampled (reduced) database to be validated. The data is then categorised based on the measurement technique that was employed—with these techniques introduced to the reader. The data is also categorised based on whether the reported enhancement in thermal conductivity exceeds that predicted by theory— with the underlying theory explained. The nanofluids that exhibit enhancement in excess of this theoretical limit are then classified as 'anomalous', whereas the remainder of the dataset is classified as 'conventional'—pertaining to their thermal behaviour. Finally, this section employs the considered thermal conductivity models to assess their accuracy. This analysis is conducted separately on the anomalous and conventional nanofluids as they exhibit idiosyncratic thermal behaviours.

The results section is followed by the discussion, in which the collected data pertaining to the abovementioned anomalous nanofluids is investigated to better characterise them. With these unique characteristics determined, we again consider the potential contribution of measurement error in the anomalous data. Further analysis of the database fails to provide evidence to support the existence of significant measurement error in these anomalous datapoints, and hence, some key potential mechanisms are explored. Based on the accuracy of the models and their underlying assumptions, some indication is given to the most probable mechanisms at play in the considered nanofluids.

The conclusion summarises the findings of the present critical analysis, in addition to making some key recommendations for future work—such as the development of a standardised experimentation protocol for nanofluid experimentation such that reliable, replicable measurements can consistently be achieved by independent researchers. Guidance is given on how to proceed with respect to investigating the presently identified anomalous alumina–water nanofluids further (in a benchmark study).

Methodology

The considered data were identified from publications (from journals that are above Q2 in the corresponding field) and were sourced using major publication databases and journal search engines (Scopus, Google Scholar, ScienceDirect and Imperial College Library). The dataset was limited to experimental data related to Al_2O_3–water nanofluids under ambient pressure, which are the most studied nanofluids and, therefore, a larger number of studies are available. The error incurred by reading data points from graphs was of the order of 1–5%. The reported nominal nanoparticle diameter (d) of the mixtures is usually based on information provided from the manufacturer and, when stated as a range, the average diameter was reported, while, when stated as lower than a given value, the reported diameter was assumed. Thermal conductivity data was sourced from 72 publications ($n = 72$ [16–87]) yielding 343 observations ($n = 343$), with evidence to support the sufficiency of this sample size presented in Sect. "Anomalous Enhancement or Measurement Error?". Box/violin plots sourcing data from fewer than 5 publications ($N < 5$) were treated as statistically insignificant, and hence were not plotted [88]. The optimal bin width for use in the reported bar plots was calculated from the formula of Scott [89]. A custom-made Python code was used to conduct the data processing and statistical analyses. Python v3.9.13 was employed with the open-source libraries numpy (v1.21.5), matplotlib (v3.5.2), scipy (v1.9.1), pandas (v1.4.4), seaborn (v0.11.2) and sklearn (v1.0.2)."

Several issues may be present in the identified database. Since the characteristics of the nanofluids of each study are unique (stability, concentration, nominal and agglomerate diameter), analysis of the database without any preliminary data processing would bias the results in favour of publications from which a greater number of observations (n) were sourced. Furthermore, potential trends may have originated from a single publication, and hence would be uncorroborated and potentially be subject to systematic error. Alternatively, numerous points from a single study could obfuscate a corroborated trend between several independent publications. These issues were overcome by randomly sampling an equivalent number of observations from each publication to form a reduced dataset, thus weighing the results of each publication equally. The number of observations randomly sampled from each publication (n'_r) was determined such that the

resulting reduced dataset did not vary significantly when the sampling procedure was repeated (yielding n_r observations from N_r publications). In processing the dataset in this way, it was assumed that each publication was independent, whereas several publications may have originated from the same groups/authors.

Data from both α and γ crystalline phases of Al_2O_3 nanoparticles were collated. As discussed later in Sect. "Characterising Anomalous Nanofluids", depending on the crystalline phase of alumina used, the isoelectric point (IEP) changes, which affects nanofluid stability [13], and hence may influence the nanofluid thermal conductivity (for example, Xie et al. [51] found thermal conductivity enhancement to increase as one adjusted the pH of the nanofluid further from the IEP). However, the crystallographic phase of alumina has been reported to have no effect on the thermal conductivity of alumina nanofluids [51], thus justifying the inclusion of both crystalline phases in the dataset.

Regarding the investigation of the accuracy of nanofluid thermal conductivity theoretical and semi-empirical models, only models applicable to the presently considered nanofluid were selected. These were mainly sourced from the review of Lee et al. [8], which also details the underlying assumptions and theoretical justifications of the models used herein [15, 56, 90–108]. The main assumptions required by the selected models were that the nanofluid was constituted of spherical nanoparticles and had low nanoparticle concentration. Most authors in the collated dataset verified the spherical shape of their particles via transmission electron microscopy (TEM), satisfying the former assumption. Data points obtained from nanofluids constituted of non-spherical particles were excluded, for example, Hwang et al. [61] tested an assortment of shapes, including platelets, blades and bricks.

Several models of the thermal behaviour of spherical nanoparticles in solutions were tested in the current study to assess their validity in describing experimental results. The current study did not consider some published models [8, 109], which included derivations that were dimensionally inconsistent.

Some of the models contained undefined parameters, such as empirical constants in the case of semi-empirical models and unmeasured parameters in theoretical models, such as nano-layer thermal conductivity. These were specified through curve fitting routines, i.e. tweaking undefined parameters using non-linear least squares fit methods, so that model accuracy was maximised. Some of these parameters were arbitrary coefficients, whilst some other parameters were claimed to have a physical basis by the authors. The magnitude of the parameters that were stated to have a physical basis was assessed, to verify whether they were physically sensible. In some cases, the selected magnitudes were not realistic (discussed later).

With regards to quantifying the accuracy of thermal conductivity models, the regression coefficient R^2 applies only to linear models. Given that most of the models were non-linear, an alternative approach was required. The standard error of regression (S)—also known as residual standard error—fulfils this requirement, as it is applicable to linear and non-linear regression models [110]. To satisfy the assumption of low nanoparticle concentration made by some models, only data points with volumetric concentration $\phi <$ 20 vol% were initially included in the analysis (Jeffrey [95] investigated nanofluids up to this concentration with their model which assumed low concentration). It was desired to reduce the maximum concentration used in the dataset further to omit denser nanofluids, which would exhibit increased agglomeration and larger viscosities, yielding fluids more akin to slurries as opposed to dilute colloids (recalling the definition of a nanofluid from the Introduction). It was observed that reducing the maximum concentration of the dataset from 20 to 13 vol% had no effect on the results (e.g. accuracy of the models), and hence this value was used.

The thermophysical properties of Al_2O_3 and water used for calculations are presented in Table 1. The effect of temperature on these thermophysical properties (as temperatures above ambient were considered in the dataset) was accounted for through employing the equations of Zografos et al. [111].

When computing predicted values from the considered thermal conductivity models, the sample size of the original dataset was reduced further, as for example, some models required diameter d and temperature T as additional input parameters. The resulting number of publications and total observations for these filtered datasets is presented in Table 2. Table 2 shows that the filtered datasets remain sufficiently large ($N_r > 50$, $n_r > 100$).

Results

In this section, the reduced dataset is used to visualise the distribution of the reported enhancement and quantify the most common—and hence most probable—thermal

Table 1 Thermophysical properties of Al_2O_3 and water at $T = 293$ K [112]

Property	Value
k_p/Wm^{-1} K^{-1}	42.64
K_{bf}/Wm^{-1} K^{-1}	0.613
ρ_p/kgm^{-3}	3880
ρ_{bf}/kgm^{-3}	1086.27
$c_{p,p}$/Jkg^{-1} K^{-1}	765
$c_{p,bf}$/Jkg^{-1} K^{-1}	4179
μ_{bf}/Pa s	9.93×10^{-4}

Table 2 Number of publications and observations in the reduced dataset and the resulting datasets when filtered to accommodate additional parameters

Parameters	N_r	n_r
v	67	134
v, d	64	128
v, T	52	104
v, d, T	49	98

performance expected for the considered nanofluid. The performance of the reduced dataset is then checked to verify it retains a large enough sample size to avoid significant error, in addition to repeatedly sampling the full dataset to ensure insignificant variation in the resulting reduced dataset of the considered size. Following this, the working principle for the different methods of thermal conductivity measurement employed in the nanofluids research field are introduced and explained. There have been reports of discrepancy between the different measurement methods—even for identical nanofluids, and so we categorised the data based on measurement method to investigate this issue, analysing the resulting probability distributions and parameter spaces. The concept of anomalous thermal conductivity enhancement is introduced and defined in the context of fundamental theoretical models, from which the data is classified as falling into either the mode of anomalous or conventional thermal conductivity enhancement. The performance of the considered theoretical and semi-empirical models is also investigated.

Overall thermal conductivity performance and the reduced dataset

The distribution of the reported thermal conductivity ratios of the full and reduced datasets is presented in the bar plot in Fig. 1. The reduced dataset increases the weighting towards lower enhancements of thermal conductivity (between 1 and 9%), indicating that the full dataset may have been biased towards larger enhancements ($\geq 10\%$). Considering the reduced dataset, most observations (47%) report enhancement between 0 and 4%. This value differs from the previous work [9], which obtained a modal enhancement between 5 and 9%, indicating that nanofluids other than Al_2O_3–water yield greater enhancements in thermal conductivity on average.

Sample size justification

After omitting bias from the dataset through the formulation of the reduced dataset (i.e. randomly sampling 2 observations from each publication), the effect of sample size (number of publications sampled, N_{sample}) on the distribution of the reported thermal conductivity ratios (k_{nf}/k_{bf}) was investigated in order to verify that the sample size was sufficient. The results are presented in Figs. 2a and b.

From these figures, it is seen that after sourcing data from more than 40 publications, no significant change in the probability distribution and square error is observed (max square error reduces from 24 to 5%). The repeatability of this sampling method is demonstrated in Fig. 3, where no significant change in the measured variables is observed whilst repeatedly sampling 40 publications from

Fig. 1 Bar plots (full and reduced datasets, optimal bin width) of percentage thermal conductivity enhancement for Al_2O_3–water nanofluids under atmospheric pressure, 293 K < T < 333 K. $N_r = 68$ as the data for non-spherical particle nanofluids from Hwang et al. [61] is included, reduced dataset
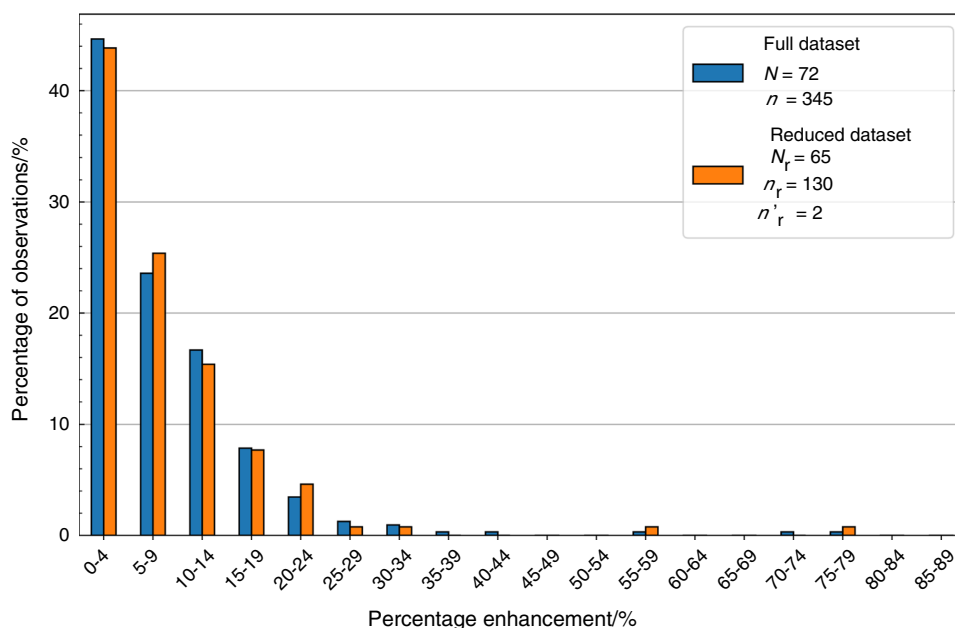
Fig. 2 Effect of randomly sampling differing numbers of publications (N_{sample}) on the **a** probability distribution of thermal conductivity ratio (k_{nf}/k_{bf}), and **b** resulting square error (with reference to the case $N_{sample} = N_r = 67$), reduced dataset
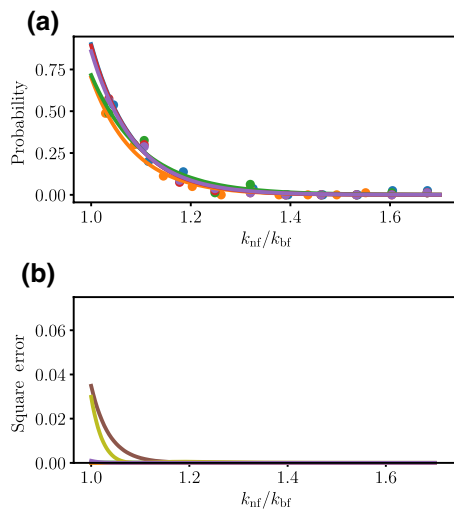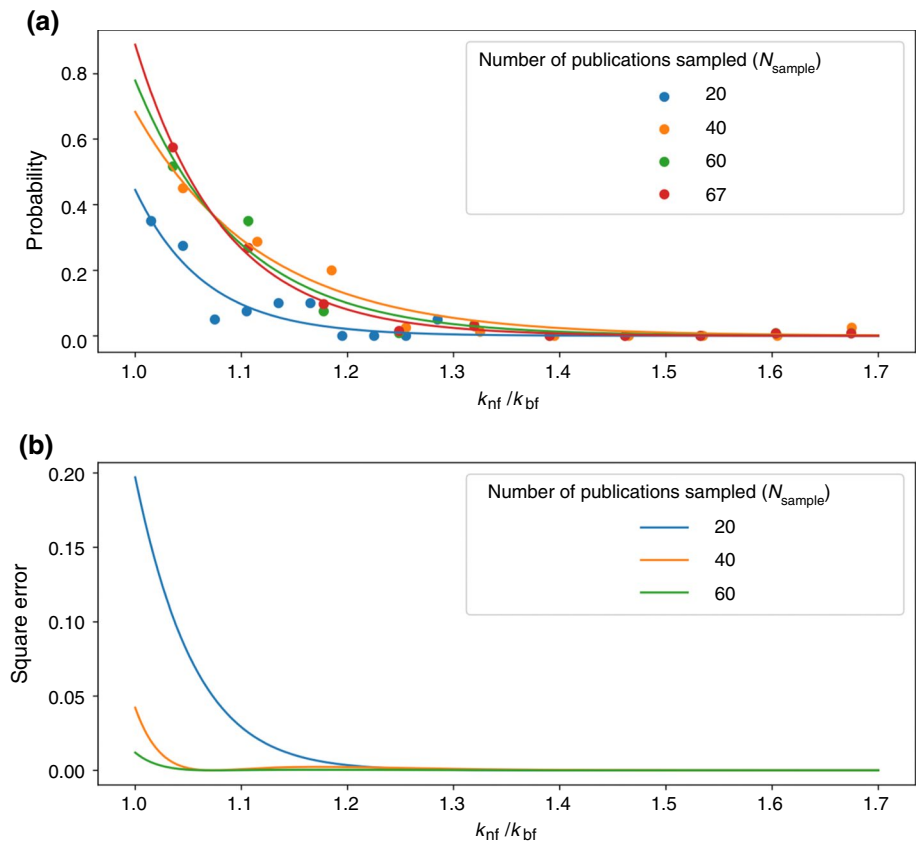

Fig. 3 Effect of repeatedly sampling 40 random publications ($N_{sample} = 40$) on the **a** probability distribution of thermal conductivity ratio (k_{nf}/k_{bf}), and **b** resulting square error (with reference to the case $N_{sample} = N_r = 67$), reduced dataset

the full dataset. Hence the reduced and presently used sample size ($N_r = 49$, Table 2) sufficiently represents the full population whilst omitting bias.

Measurement technique

As mentioned above, discrepancy has been reported between different thermal conductivity measurement techniques. These discrepancies will depend on the unique characteristics of each approach, and so an introduction to the working principle of each method is provided, in addition to consideration of the reported discrepancies in the literature. This analysis is then extended to the present data, in which the discrepancy between measurement methods for similar system parameters is investigated.

Thermal conductivity can be measured using either transient or steady-state approaches, with typical methods shown in Fig. 4. A key issue in measuring the thermal conductivity of fluids is the presence of natural convection, induced by temperature gradients during the process of sample heating. To allay this in transient applications, smaller sample sizes are used, and measurement times are minimised. In steady-state applications, thermal equilibrium is established [113, 114].

The transient hot-wire method (THW) is shown in Fig. 4a, in which the temperature rise in one or two metallic wire(s) undergoing resistive heating is measured and used to infer the thermal conductivity of the sample medium. Special attention is given to the accuracy of this measurement method in Sect. 5.2, as it is the most widely used and there
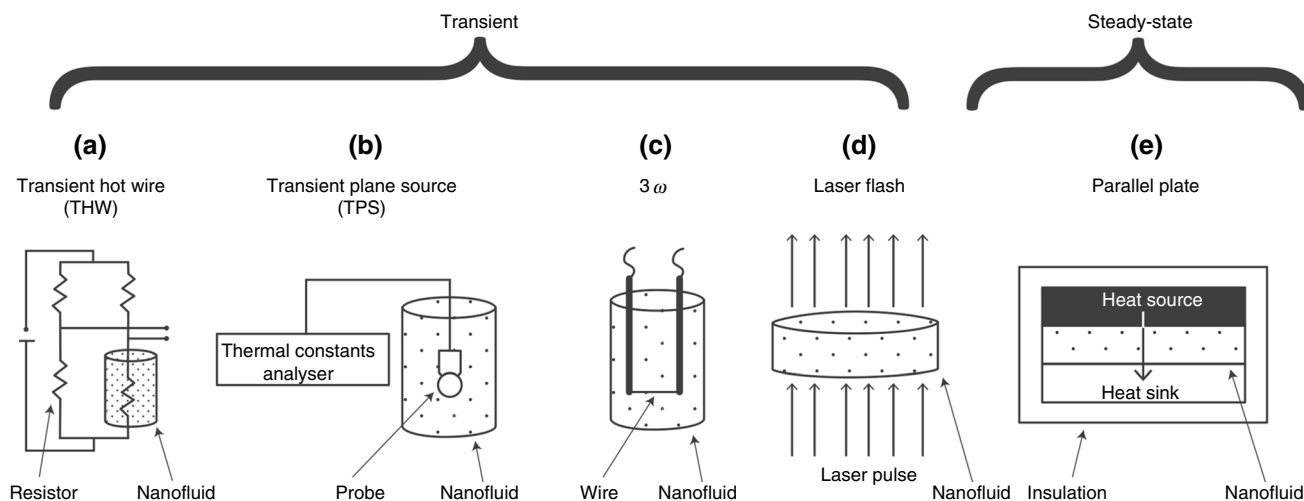
Fig. 4 Thermal conductivity measurement methods (adapted from [115])

is contention on its applicability to nanofluids. For example, for THW probes which are not electrically insulated, parasitic currents may augment the reported heat transfer measurement—but not the true physical value [14].

The transient plane source (TPS) method is shown in Fig. 4b, which operates under similar assumptions as the THW method, except that the heat source is a circular plane instead of an infinite line.

The 3ω method is shown in Fig. 4c, in which a sinusoidal electrical current of frequency ω is passed through a micron-sized thin film metal heater. Using this technique, thermal conductivity can be measured using just a droplet of sample medium [45].

The laser flash method is shown in Fig. 4d, in which the sample is heated by an energetic laser pulse from one side, and the temperature rise of the sample is measured from the other side (e.g. using infrared imaging). This method is advantageous in that the heating of the sample occurs on the timescale of nanoseconds, eliminating contributions from natural convection [115].

The steady-state parallel plate method is shown in Fig. 4(e) (concentric cylinders can also be used). Upon the establishment of an equilibrated temperature gradient, thermal conductivity can be computed from Fourier's Law. However, in practise it is difficult to perfectly insulate the system and prevent heat losses [114].

The 3ω and TPS methods are disadvantaged in that they usually require calibration and lack a strong theoretical basis [113]. Some authors have attempted to compare the measured thermal conductivities obtained by different methods for identical nanofluids. For example, Buonomo et al. [116] compared the laser flash and TPS methods and found their results to be similar. Aparna et al. [117] compared the laser flash and THW methods and found the latter to yield greater

enhancements in nanofluid thermal conductivity. Using MDS results, they argued that the THW method is more reliable than the laser flash method, as the small length scale of the laser flash system (0.3 mm in their case) reduces the collision flux of the nanoparticles in the sample across the thermal boundary layer, thus inhibiting heat transfer. Further details on the different methods of measuring thermal conductivity are presented in a review by Xu et al. [118].

The data was categorised by the experimental technique used to acquire the measurements, with the results presented in Fig. 5 (where $N_r > 4$). The measurement techniques were the THW method, the THW method with an electrically conductive sensor (THWe) and the transient plane source method (TPS). It is important to note that although some THW devices are stated to be electrically insulated (e.g. KD2 Pro KS-1 probe), this does not guarantee their electrical insulation in use (e.g. a Teflon coating is sprayed to the probe surface before use [93]; however, how this coating performs/deteriorates is unknown). The most commonly used method for thermal conductivity measurements in nanofluids was THW ($\approx 67\%$ of publications), followed by THWe ($\approx 10\%$) and TPS ($\approx 8\%$). The greatest modal enhancement was reported by the TPS method (5–9%, 60% of observations). Identical modal enhancements were reported by the THW and THWe methods (0–4%), although the THWe method had a greater proportion of observations in this range and yielded no observations of extreme enhancement ($> 40\%$), even when considering the full dataset.

It appears that different measurement techniques might be leading to differently reported results, which could be explained by differences in particle concentrations and sizes. Figure 6 shows the distribution of volumetric concentrations and particle sizes categorised by measurement method, where it is seen that the concentrations are

Fig. 5 Bar plot of measurement method dependency of percentage thermal conductivity enhancement for Al_2O_3–water nanofluids under atmospheric pressure, 293 K < T < 333 K, reduced dataset ($n'_r = 2$)
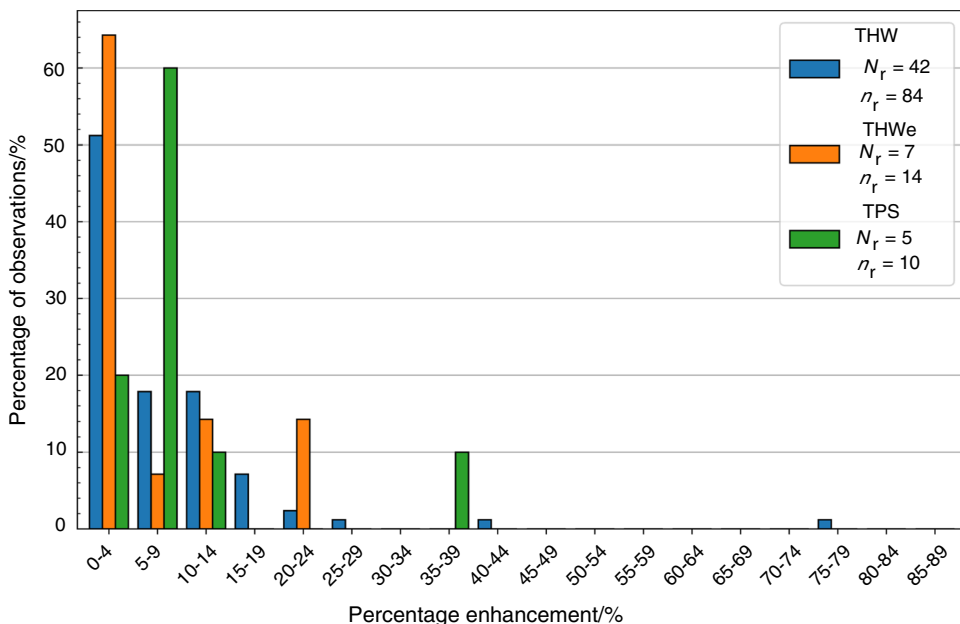

Fig. 6 Violin plots showing the parameter space for the considered measurement methods for Al_2O_3–water nanofluids under atmospheric pressure, 293 K < T < 333 K, reduced dataset ($n'_r = 2$). The parameter spaces are seen to be sufficiently similar between the different measurement methods, and hence based on this one would expect a similar distribution in reported thermal enhancement in Fig. 5 between the different methods
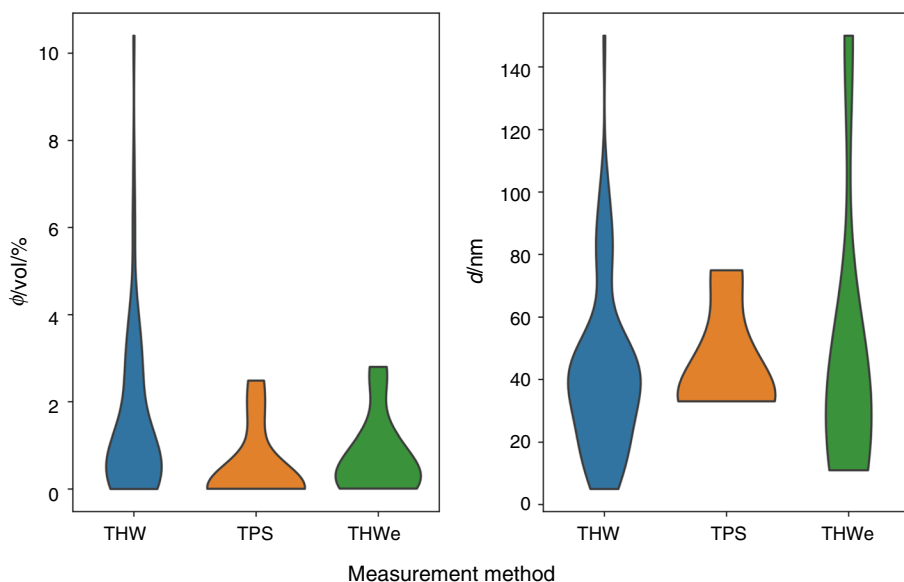
similar; however there is some discrepancy between the particle sizes used, specifically between THW(e) and TPS. Overall, this suggests that the particle concentrations and sizes of the nanofluids considered by each measurement technique were sufficiently similar to expect comparable measured thermal conductivity values. Thus, our findings agree with the literature, in that a discrepancy does exist between thermal conductivity measurement methods in the context of nanofluids. However, the differing stabilisation and dispersion of these nanofluids will also contribute to the discrepancies, as although the concentrations and

particle diameters are similar, the particle size distributions can be expected to vary.

Anomalous thermal conductivity enhancement

For an enhancement in nanofluid thermal conductivity to be deemed 'anomalous', it must exceed the upper bound of effective medium theory (EMT), given by the Hashin–Shtrikman (HS) upper bound [94, 119]. The lower HS bound reduces to Maxwell's equation [15] and represents the worst-case scenario from the perspective of EMT
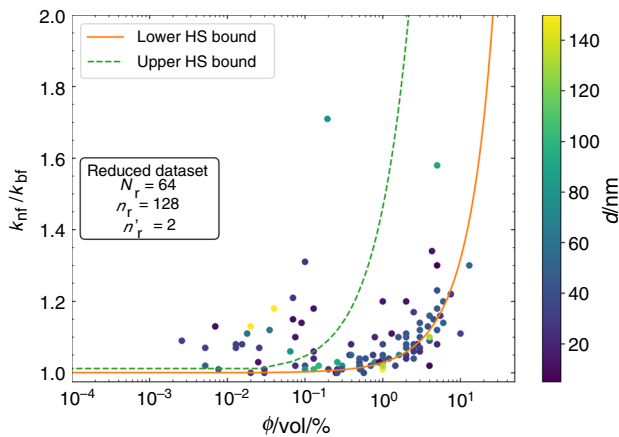
Fig. 7 Plot of nanofluid volumetric concentration versus thermal conductivity ratio (k_{nf}/k_{bf}) for Al_2O_3–water nanofluids under atmospheric pressure, including Hashin–Shtrikman bounds and colour map of nanoparticle nominal diameter, 293 K < T < 333 K, $N_r = 64$, reduced dataset

(uniformly dispersed noninteracting spherical particles). Figure 7 shows that the thermal conductivity of the investigated nanofluids can exceed the upper HS bound at low volumetric concentrations ($\phi \leq 0.2$ vol%), lie within the bounds at intermediate concentrations (0.2 vol% < ϕ < 1.0 vol%) and lie below the lower bound at higher concentrations (ϕ > 1.0 vol%). Nanofluids falling within theoretical predictions are classified as conventional nanofluids herein. Figure 7 also includes a colour map of the manufacturer stated nominal nanoparticle diameter (d) for each data point, which shows that the usage of small nanoparticle diameters does not guarantee anomalous enhancement and that anomalous enhancement was reported even for quite large particles ($d \approx 100$ nm). No clear dependence on d is observed, making it difficult to predict the nanofluid thermal conductivity based on this parameter. Since the reduced dataset was used, these results are unbiased and corroborated by several authors (12 independent publications reported anomalous enhancement for $\phi \leq 0.2$ vol%). One could argue that these anomalous data points could lie within the HS bounds, when accounting for the uncertainty in their measurement. Tertsinidou et al. [113] collated similar data (thermal conductivity of Al_2O_3–water nanofluids under ambient conditions), noting the measurement uncertainty where reported. This ranged from 0.05 to 5%. Even taking the worst case ($\pm 5\%$), most of the observed data points still lie beyond the limit of uncertainty (> 10%). In fact, it has been reported that uncertainties in nanofluid thermal conductivity measurements are mainly systematic, and hence eliminated on computation of the effective thermal conductivity ratio (i.e. enhancement) [14]. Alternatively, it could be argued that these anomalous data points are caused by higher system temperatures; however all the anomalous data points displayed in this figure were

measured at ambient temperatures (298 K < T < 301 K), thus negating the possibility of higher system temperatures augmenting the enhancement. Hence, assuming the underlying experimental and measurement methods were sensible, these data points appear to indicate an anomalous, i.e. unexpected, behaviour. These observations of anomalous enhancement at low concentrations have also been reported for other nanofluids by several authors [8, 47].

Theoretical/semi-empirical modelling

The data points of anomalous enhancement (herein denoted also as nanofluids behaving under the mode of anomalous thermal conductivity enhancement or anomalous nanofluids) exhibited in Fig. 7 elude all the tested nanofluid thermal conductivity models, even when the fitted parameters are based on the entire reduced dataset (conventional and anomalous data points). To improve accuracy, data points of anomalous enhancement (exceeding the upper HS bound) were omitted and modelled separately. Segregating the data into two regions, namely anomalous/conventional modes, is a good tool for analysis. However, it poses the difficult issue of predicting in which mode a given formulated nanofluid falls under. Indicative characteristics of anomalous mode nanofluids are presented in Sect. "Characterising Anomalous Nanofluids".

Table 3 lists the theoretical and semi-empirical models investigated in this work. Full equations and parameters are provided, with further details available in the original publications. Constants are also provided, and indication is provided for 'fitted' constants—i.e. obtained via statistically fitting a model function against the measured experimental data. The underlying assumptions behind each model (e.g. spherical particles) and the mechanism type (e.g. nanoconvection) are also listed. From this information, the accuracy of each model (under each of the two enhancement modes) was quantified by computing the standard error of regression, S (representing the error in enhancement fraction, e.g. 0.01 indicates a 1% error between predicted and observed enhancement). For the conventional mode these values are visualised in Fig. 8, quantifying the accuracy of the tested models.

With regards to the fitted parameters in Table 3, the fitted value of β in the Jang and Choi model was sensible, as $\beta \sim$ 0.01 [101] (β is defined as the ratio between effective nanoparticle conductivity—reduced by interfacial resistance—to that of the nanoparticle alone, ranging between 0 and 1). The order of magnitude for the parameters in the Koo and Kleinstreuer function ($f(v, T)$) is larger than what they obtained in their work for a CuO nanofluid [102], which may be due to the differing definitions of ϕ and volumetric fraction (v) used. The value of τ (particle relaxation time) in the Yang model is of a sensible order of magnitude [104]. Regarding

Table 3 Employed thermal conductivity models and their standard errors of regression (S). Fitted parameters and standard errors correspond to conventional nanofluids, whilst the aforementioned values in brackets correspond to anomalous nanofluids

Model type	Model	Equation	Standard Error of Regression, S	Assumptions
Effective medium theory ↓	Maxwell [15]	$k_{nf}/k_{bf} = \dfrac{k_p + 2k_{bf} + 2v(k_p - k_{bf})}{k_p + 2k_{bf} - v(k_p - k_{bf})}$	0.06 (0.1)	Spherical particles, low concentration
	Turian et. al. [90]	$k_{nf}/k_{bf} = k_{bf}^{1-v} k_p^v / k_{bf}$	0.08 (0.07)	Randomly dispersed solid inclusions in liquid
	Maxwell Limit [56, 91]	$k_{nf}/k_{bf} = 1 + 3v$	0.06 (0.15)	Spherical particles, low concentration
	Bruggeman [92, 93]	$k_{nf}/k_{bf} = \dfrac{1}{4k_{bf}}\left[(3v-1)k_p + (2-3v)k_{bf}\right] + \dfrac{1}{4}\sqrt{\Delta}$ $\Delta = (3v-1)^2(k_p/k_{bf})^2 + (2-3v)^2 + 2(2+9v-9v^2)(k_p/k_{bf})$	0.07 (0.15)	Spherical particles
	Hashin-Shtrikman lower bound [94]	$k_{nf}/k_{bf} = 1 + \dfrac{3v(k_p/k_{bf}-1)}{3k_p/k_{bf} - v(k_p/k_{bf}-1)}$	0.06 (0.13)	Spherical particles
	Hashin-Shtrikman upper bound [94]	$k_{nf}/k_{bf} = (k_p/k_{bf})\left[1 - \dfrac{3(1-v)(k_p/k_{bf}-1)}{3k_p/k_{bf} - v(k_p/k_{bf}-1)}\right]$	0.46 (0.14)	Spherical particles
	Jeffrey [95]	$k_{nf}/k_{bf} = 1 + 3\beta v + v^2\left(3\beta^2 + \dfrac{3\beta^3}{4} + \dfrac{9\beta^3}{16}\dfrac{\chi+2}{2\chi+3} + \dfrac{3\beta^4}{2^6}\right)$ $\chi = k_p/k_{bf}$ $\beta = (\chi-1)/(\chi+2)$	0.06 (0.14)	Spherical particles, low concentration
Nano-layer/interfacial resistance ↓	Nan et. al. [96, 97]	$k_{nf}/k_{bf} = \dfrac{k_p(1+2\alpha)+2k_{bf}+2v\left[k_p(1-\alpha)-k_{bf}\right]}{k_p(1+2\alpha)+2k_{bf}-v\left[k_p(1-\alpha)-k_{bf}\right]}$ $\alpha = R_K k_{bf}/r$, $R_K = 1.09 \times 10^{-8} m^2\, KW^{-1}$ [108]	0.07 (0.14)	Spherical particles, low concentration, interfacial resistance
	Xue and Xu [98]	$\left(1-\dfrac{v}{\chi}\right)\dfrac{\alpha-k_{bf}}{2\alpha+k_{bf}} + \dfrac{v}{\chi}\dfrac{(\alpha-k_l)(2k_l+k_p)-\chi(k_p-k_l)(2k_l+\alpha)}{(2\alpha+k_l)(2k_l+k_p)+2\chi(k_p-k_l)(k_l-\alpha)} = 0$ $\chi = \left(\dfrac{r}{r+\delta}\right)^3$ $\alpha = k_{nf}/k_{bf}$ $\delta = 3$ nm $k_l = 5\,\text{W m}^{-1}\,\text{K}^{-1}$	0.29 (0.14)	Spherical particles, nano-layer
	Yu and Choi [99]	$k_{nf}/k_{bf} = \dfrac{k_p+2k_{bf}+2(k_p-k_{bf})(1+\gamma/r)^3 v}{k_p+2k_{bf}-(k_p-k_{bf})(1+\gamma/r)^3 v}$ $\gamma = 0.01(T - 273)r^{0.35}$ /nm	0.06 (0.14)	Spherical particles, nano-layer
	Xie et. al. [100]	$k_{nf}/k_{bf} = 1 + 3\Theta v_T + \dfrac{3\Theta^2 v_T^2}{1-\Theta v_T}$ $v_T = v(1+\gamma)^3$ $\gamma = \delta/r$ $\Theta = \dfrac{\frac{k_l-k_{bf}}{k_l+2k_{bf}}\left[(1+\gamma)^3 - \frac{(k_p-k_l)k_{bf}+2k_l}{k_p+2k_l}\right]}{(1+\gamma)^3 + 2\frac{k_l-k_{bf}}{k_l+2k_{bf}}\frac{k_p-k_l}{k_p+2k_l}}$ $\delta = 3$ nm, $k_l = 5\,\text{W m}^{-1}\,\text{K}^{-1}$ [96]	0.20 (0.14)	Spherical particles, nano-layer

Table 3 (continued)

Model type	Model	Equation	Standard Error of Regression, S	Assumptions
(Brownian motion induced) nanoconvection↓	Jang and Choi [101]	$k_{nf}/k_{bf} = (1 - v) + \beta(k_p/k_{bf})v + C_1(d_{bf}/d)Re_d^2 Pr v$ $\beta = 0.0436(3.36)$(fitted) $C_1 = 18 \times 10^6$ $d_{bf} = 0.384$ nm $Re_d = \overline{C}_{R.M.} d/v$ $\overline{C}_{R.M.} = D_0/l_{bf} /s^{-1}$ $l_{bf} = 0.738$ nm $D_0 = k_B T/3\pi\mu d /nm\,s^{-1}$	0.05 (0.12)	Spherical particles, interfacial resistance, nanoconvection
	Koo and Kleinstreuer [102]	$\dfrac{k_{nf}}{k_{bf}} = \dfrac{k_p + 2k_{bf} + 2v(k_p - k_{bf})}{k_p + 2k_{bf} - v(k_p - k_{bf})} + \dfrac{1}{k_{bf}}(5 \times 10^4)\beta v \rho_p c_{p,p}\sqrt{\dfrac{k_B T}{\rho_p d}}f(v, T)$ $\beta = 0.0137(100\phi)^{-0.8229}$ for $\phi < 1$ vol.% else $\beta = 0.0017(100\phi)^{-0.0841}$ $f = \left[-1.32 \times 10^5 v + 1.07 \times 10^4\right]T + 3.86 \times 10^7 v - 3.15 \times 10^6 \left(\left[5.29 \times 10^6 v + 6.47 \times 10^5\right]\right.$ $\left. T + -6.57 \times 10^{11} v + 3.35 \times 10^8\right)$(fitted, form from [100])	0.04 (0.10)	Spherical particles, nanoconvection
	Prasher [103]	$k_{nf}/k_{bf} = (1 + ARe^m Pr^{0.33}v)\left[\dfrac{k_p + 2k_{bf} + 2v(k_p - k_{bf})}{k_p + 2k_{bf} - v(k_p - k_{bf})}\right]$ $Re = \dfrac{1}{v}\sqrt{\dfrac{18k_B T}{\pi \rho_p d}}$ $A = -458(2.11 \times 10^{-5})$(fitted), $m = 95.7(-1.08)$(fitted)	0.05 (0.07)	Spherical particles, nanoconvection
	Yang [104]	$k_{nf}/k_{bf} = \dfrac{k_p + 2k_{bf} + 2v(k_p - k_{bf})}{k_p + 2k_{bf} - v(k_p - k_{bf})} + 157.5 v c_{p,bf} u_p^2 \tau / k_{bf}$ $u_p = \sqrt{\dfrac{3k_B T}{m_p}} /nm\,s^{-1}$ $m_p = $ mass of one particle $= \rho_p \cdot \frac{4}{3}\pi r^3 /kg$ $\tau = 5.25 \times 10^{-11}$ s$(4.45 \times 10^{-8}$ s)(fitted)	0.06 (0.14)	Spherical particles, nanoconvection

Table 3 (continued)

Model type	Model	Equation	Standard Error of Regression, S	Assumptions
Combined ↓	Ren [105]	$k_{nf}/k_{bf} = 1 + f(Pe) + 3\Theta\nu_T + \frac{3\Theta^2\nu_T^2}{1-\Theta\nu_T}$ $\nu_T = \nu(1+\gamma)^3$ $\gamma = \delta/r$ $\Theta = \dfrac{\frac{k_l-k_{bf}}{k_l+2k_{bf}}\left[(1+\gamma)^3 - \frac{(k_p-k_l)(k_{bf}+2k_l)}{(k_p+2k_l)(k_{bf}-k_l)}\right]}{(1+\gamma)^3 + 2\frac{k_l-k_{bf}}{k_l+2k_{bf}}\frac{k_p-k_l}{k_p+2k_l}}$ $f(Pe) = 0.0556Pe + 0.1649Pe^2 - 0.0391Pe^3 + 0.0034Pe^4$ $Pe = \frac{\bar{u}L_c\,\nu_T^{0.75}}{\alpha_{bf}}$ $\bar{u} = \sqrt{\frac{3k_B T}{m_c}}\,/\,\mathrm{nm\,s^{-1}}$ $m_c = \frac{4}{3}\rho_p\pi r^3\left\{\frac{\rho_l}{\rho_p}\left[\left(1+\frac{\delta}{r}\right)^3-1\right]+1\right\}/\mathrm{kg},\ \rho_l = \rho_{bf}/\mathrm{kg\,m^{-3}}$ $\delta = 3\,\mathrm{nm},\ k_l = 5\,\mathrm{W\,m^{-1}\,K^{-1}}[96],\ \alpha_{bf} = \frac{k_{bf}}{\rho_{bf}c_{p,bf}}$	0.06 (0.11)	Spherical particles, nano-layer, nanoconvection
	Dolatabadi et. al. [106]	$k_{nf}/k_{bf} = (1-\nu) + (k_{pe}/k_{bf})\nu + C_1(n_l d_{bf}/d)\left[2 + 0.4Re_d^{1/2} + 0.06Re_d^{2/3}\right]Pr^{-0.6}\nu(\mu_\infty/\mu_s)^{1/4}$ $Re_d = \overline{C}_{R.M.}\,d/\nu$ $\overline{C}_{R.M.} = D_0/l_{bf}\,/\mathrm{s^{-1}}$ $k_{pe} = \dfrac{[2(1-\gamma_r)+(1+\beta_r)^3(1+2\gamma_r)]\gamma_r k_p^*}{-(1-\gamma_r)+(1+\beta_r)^3(1+2\gamma_r)}$ $k_p^* = 2r/(R_K + 2r/k_p)$ $\gamma_r = k_{nl}/k_p^*$ $\beta_r = t/r$ $t = n_l d_{bf}\,/\mathrm{nm}$ $k_{nl} = \dfrac{t}{\left[r(r+t)\int_r^{r+t}(r'^2\overline{k_{nl}(r')})dr'\right]}$ $\overline{k_{nl}(r')} = k_p^* + \frac{k_{bf}-k_p^*}{1-e^m}\left[1 - e^{\frac{m(r'-r)}{t}}\right]$ $C_1 = \frac{3}{\psi}-1,\ \psi = 1,\ d_{bf} = 0.384\,\mathrm{nm},\ n_l = 2.7,\ d_f = 0.384\,\mathrm{nm},\ R_K = 1.09\times10^{-8}\,\mathrm{m^2\,KW^{-1}},$ $l_{bf} = 0.738\,\mathrm{nm},\ \mu_\infty/\mu_s = 2.2\ [106]$	0.08 (0.16)	Spherical particles, interfacial resistance, nano-layer, nanoconvection
Other	Murshed [107]	$k_{nf}/k_{bf} = \dfrac{\left[1+0.27\gamma^{4/3}\left(\frac{k_p}{k_{bf}}-1\right)\right]\left[1+\frac{0.52\nu}{1-\nu^{1/3}}\left(\frac{k_p}{k_{bf}}-1\right)\right]}{1+\gamma^{4/3}\left(\frac{k_p}{k_{bf}}-1\right)\left(\frac{0.52\nu}{1-\nu^{1/3}}+0.27\nu^{1/3}+0.27\right)}$	0.45 (0.13)	Geometric structure, implicitly accounts for particle size by characterising chain-like structures through concentration (i.e. interparticle distance)

the fitted parameters in the Prasher model, the values suggested in their work ($A = 40,000$ and $m = 2.5$ [103]) were used both as fixed parameters and initial guesses for the fitted parameters. In the former case (using the values as fixed parameters), this yielded low prediction accuracy, whilst, in the latter case (initial guesses for the statistical model), although the accuracy was improved, values markedly differed from their results. The final fitted parameter was the nano-layer density, ρ_l, in the Ren et al. model [105]. The predicted thermal conductivity ratio was found to be insensitive to ρ_l, hence $\rho_l = \rho_{bf}$ was assumed.

For the conventional nanofluids, it is seen that the model of Koo and Kleinstreuer [102] yields the best accuracy (error of 4%), significantly outperforming the other considered models (the next best model was that of Jang and Choi [101], with an error of 5%). Despite this, even the models exhibiting a 4% error in predicting thermal behaviour may have high uncertainty to use in predicting behaviours of such fluids in practice; especially when considering a necessary added safety factor to avoid criticality within certain applications of interest (e.g. nuclear).

Repeating the above analysis for the anomalous nanofluids, the values of the fitted parameters and accuracies are provided in Table 3 enclosed in brackets. For these nanofluids, the model of Prasher et al. [103] was most accurate (7.5% error), followed by the model of Koo and Kleinstreuer [102] (10% error) and Jang and Choi [101] (10.5% error). The accuracies are represented visually in Fig. 9, where it is seen that overall, most of the tested models were severely inaccurate (errors above 10%). As expected, the accuracy of the HS upper bound exceeds that of the lower bound, and other EMT models, as the anomalous data points lay above the HS upper bound. Investigation of the fitted parameters revealed them to be less physically sensible than those obtained for the conventional nanofluids. For example, the value of β in the Jang and Choi model was 3.36 for anomalous nanofluids, whereas Jang and Choi suggested a value ~ 0.01 to be sensible [101] (recall that β should range between 0 and 1). This raises questions as to whether the models contain enough of the fundamental physics to be able to predict certain colloid thermal behaviours or whether the models might have been a result of a forced curve fitting correlation.

The presented findings may suggest that the physical underlying mechanisms of the most accurate models are responsible for the observed conductivity enhancement. As such, conventional enhancement can be attributed to nanoconvection (from the model of Koo and Kleinstreuer [102]), whilst anomalous enhancement can also be attributed to nanoconvection (from the model of Prasher et al. [103]). However, the accuracy of these models is more likely to be attributed to their statistical fitting to the data opposed to the correctness of their underlying assumptions, further justified by the marked difference in the magnitudes

of the fitted parameters compared to those reported in their inception. The model of Jang and Choi [101] was found to hold similar errors for both nanofluid types (5 and 10% for conventional and anomalous respectively), although it has two fitted parameters (β and C_1), which are simply linear proportionality constants opposed to the non-linear equations (with coefficients to be statistically fitted) employed by other models. Recalling that β is defined as the ratio of the effective nanoparticle thermal conductivity (accounting for interfacial resistance) to that of the nanoparticle alone [101], the larger value obtained for the anomalous nanofluid ($\beta \sim 3$)—following the theoretical basis of the parameter—indicates the non-physical case of interfacial resistance causing a threefold enhancement in effective nanoparticle thermal conductivity. Additional consideration to this observation is given in Sect. 5.3.

Overall, it has been shown that, even when fixing the nanoparticle and basefluid material and system conditions (temperature, pressure), accounting for d and T and using statistical fitting leads to roughly 5% error in the thermal conductivity enhancement of the considered nanofluids.

This finding is expected to be due to three major factors:

(1) Significant gap in the theoretical understanding of nanofluid thermal conductivity (physical mechanisms, dependence on system parameters).

(2) Lack of consideration of other system parameters that have significant effects on the effective thermal conductivity, e.g. nanofluid suspension stability, which ultimately determines the true size of the nanoparticle clusters (d_m). These parameters are not frequently reported, since they are hard to measure and require applying DLS and TEM techniques to characterise the nanoparticles present in the suspension. Even when such measurements are available, these may be highly variable, since the extent of nanoparticle agglomeration can change during nanofluid preparation, experimentation, sampling and measurement.

(3) Errors of the used measurement techniques (considered in Sect. "Anomalous Enhancement or Measurement Error?").

Discussion

In this section, the anomalous nanofluids that have been identified in the previous section are investigated further to quantify their characteristics. For example, to formulate a nanofluid that exhibits anomalous thermal behaviour, is it better to use low or high nanoparticle concentration? Should one adjust the nanofluid pH or employ surfactants to stabilise the suspension? With these questions answered, we can better understand what system conditions are conducive to
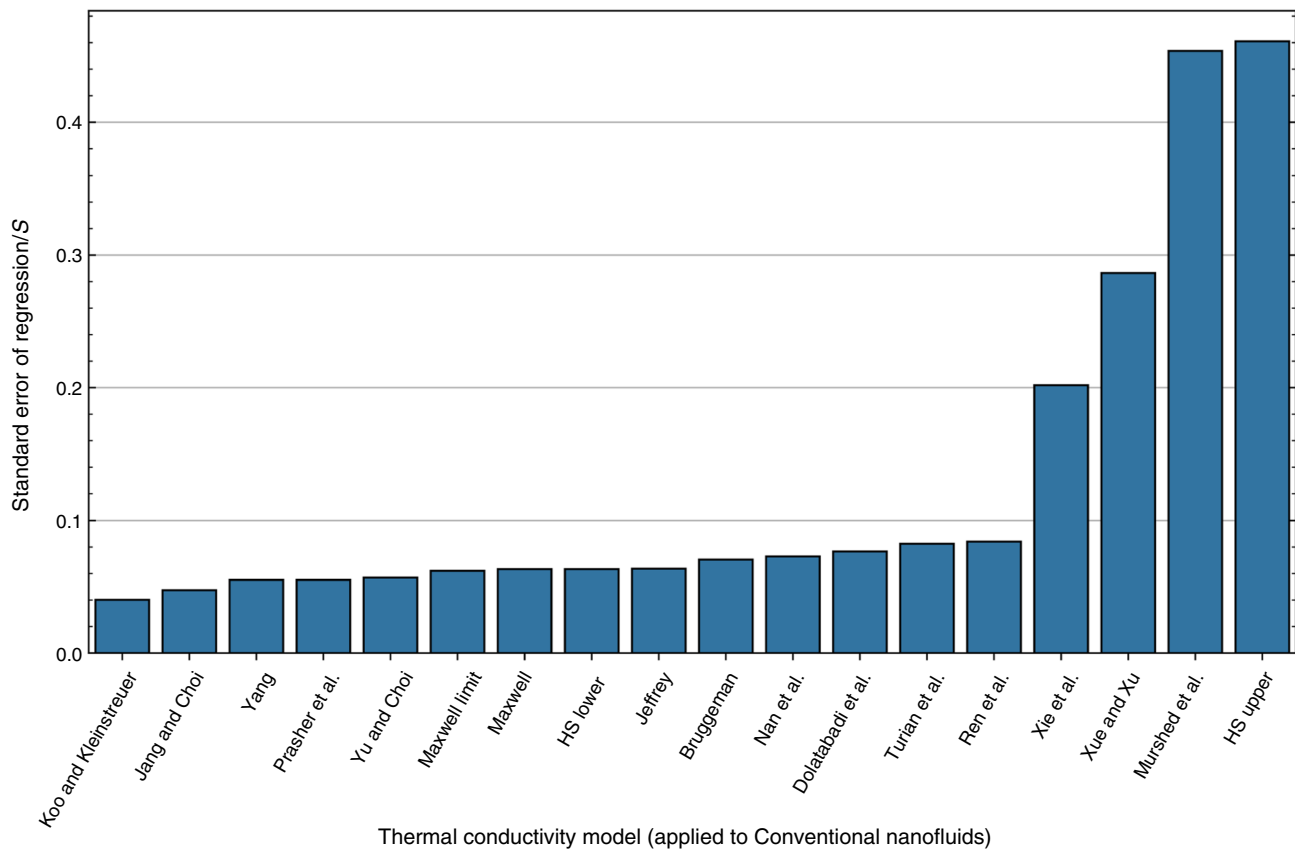
Fig. 8 Accuracy of the tested thermal conductivity models for conventional nanofluids, descending order by accuracy (lower value of S is better)

augmenting nanofluid heat transport. Further, these characteristics will inform on the underlying causes of the observed enhancements, aiding in elucidating the fundamental mechanisms and enabling theoretical development.

With the unique characteristics of these anomalous nanofluids understood, we then return to the issue of measurement error. Special attention is given to the THW method as it is the most used, where we consider the issues of parasitic current and the applicability of the technique to nanofluids. It is concluded that there is insufficient evidence to rule out anomalous thermal conductivity enhancement, warranting the exploration of the proposed mechanisms. These mechanisms are studied in the context of the above findings, enabling novel conclusions to be drawn on the most probable mechanism (nanoconvection).

Characterising anomalous nanofluids

Elaborating on the findings of Sect. "Theoretical/Semi-Empirical Modelling", the lower HS bound corresponds to uniformly dispersed spherical particles with no agglomerates or structures, whereas the upper bound represents a nanofluid with nanoparticles forming the continuous phase

and dominant conduction paths. For lower volumetric concentrations, this can only be achieved through the formation of highly efficient fractal (chain-like) structures [119]. The existence of these chain-like structures and their influence on thermal conductivity has been reported experimentally. Nimdeo and Srivastava [21] observed the formation of chain-like structures at low concentrations, whilst, conversely at higher concentrations, the chain-like structures disappeared and were replaced with larger agglomerates. Further, experiments with magnetic Fe_3O_4 nanofluids have demonstrated the impact of orienting the nanoparticle chain structures parallel and perpendicular to the applied heat flux, approximating to parallel (HS upper bound) and series (HS lower bound) thermal conductivities [119, 120].

The anomalous thermal conductivity enhancement above the upper HS bound observed in Fig. 4 is surprising. According to Eapen et al. [119], this bound is seldom exceeded and, in such a case, further information is required on the "statistical variation of the dispersed medium". The formation of chain-like structures for dilute nanofluids is insufficient to explain the anomalous enhancement alone, since it can only enhance thermal conductivity up to the theoretical maximum of the effective medium theory (upper HS bound) [119].
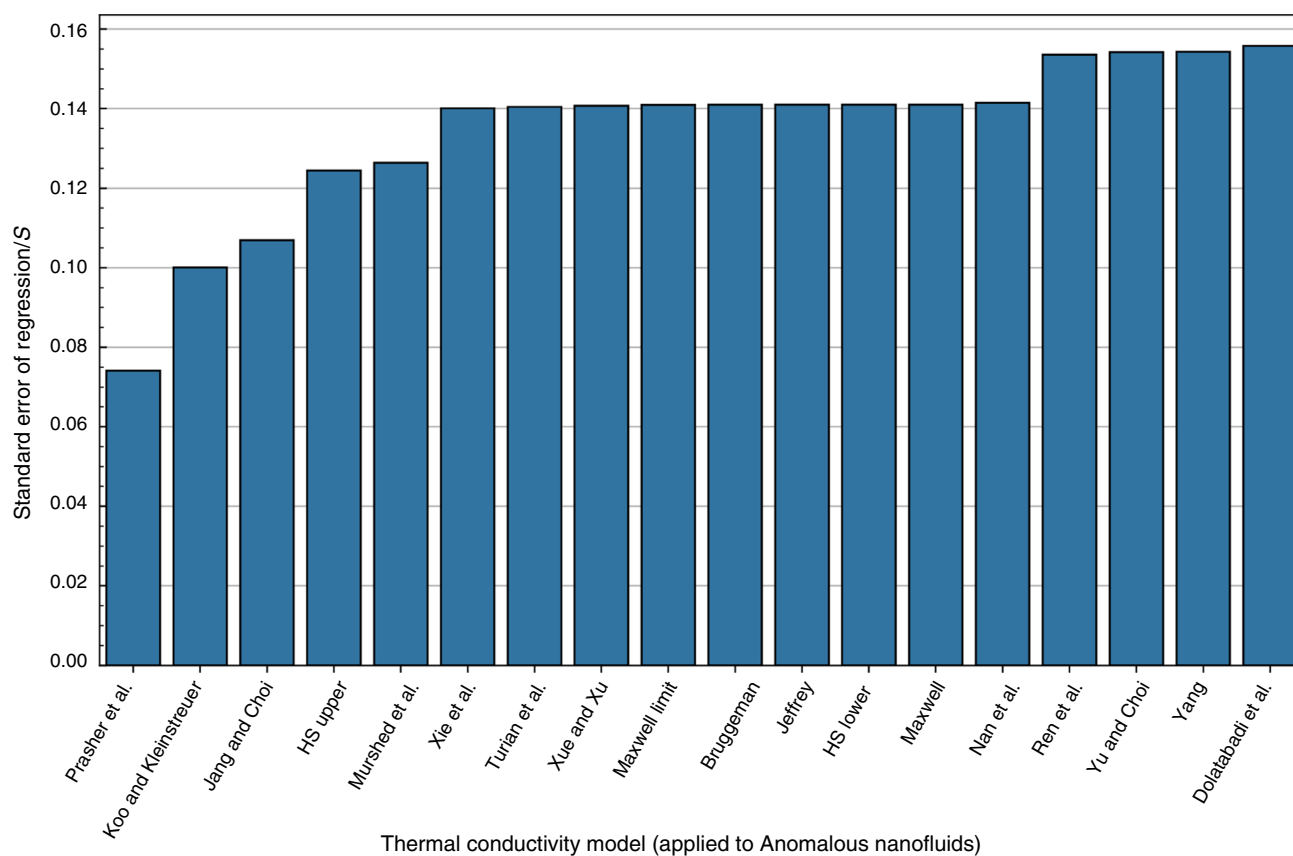
Fig. 9 Accuracy of the tested thermal conductivity models for anomalous nanofluids, descending order by accuracy (lower value of S is better)

Hence, unless measurement errors are responsible for these observations (explored in Sect. 5.2), evidence is provided for the existence of anomalous mechanisms.

Segregation of the data in Sect. 4.5 proved useful in improving the accuracy of the tested models. However, as mentioned previously, determining whether one has formulated an anomalous nanofluid remains an issue. This is because one can formulate a nanofluid with a concentration less than 0.2 vol%, and yet not observe anomalous enhancement, as can be seen in Fig. 7. Thus, indicative characteristics of nanofluids that increase the probability of observing anomalous enhancement are investigated. This is achieved by characterising the suspension stability, measurement technique, nanoparticle concentrations and nominal diameters of nanofluids in the region of anomalous enhancement ($\phi < 0.2$ vol%). The resulting analyses are presented in Figs. 10a, b and 11 respectively.

Figure 10 visualises the characteristics of the anomalous and non-anomalous nanofluids. The nanofluids are categorised by their stability characteristics in Fig. 10a, which also considers the *type* of stability realised—either through pH adjustment or the employment of a surfactant (electrostatic versus steric). Figure 10b categorises the nanofluids based on measurement technique, to ascertain whether

measurements of anomalous thermal enhancement could be linked to certain measurement methods and vice versa for non-anomalous measurements. From Fig. 10a, a similar proportion of both anomalous and conventional nanofluids were characterised as stable ($\approx 68\%$). The criterion for suspension stability was either (a) A stable zeta potential measurement (> 30 mV [121], achievable for example by extensive ultrasonication [20]) or, (b) Measured nanofluid pH far from the IEP of alumina (9.1 for $\gamma - Al_2O_3$ [86], 7.7–7.9 for $\alpha - Al_2O_3$ [13, 122], achievable with or without pH controllers) or, (c) The employment of a surfactant. It is important to note that the remaining 30% of (non-)anomalous nanofluids were not necessarily unstable, only that information regarding their stability was not provided in the publications they originated from (in other words, they may have indeed been stable). Interestingly, none of the conventional nanofluids had stable pH values, whilst a significant proportion (40%) of the anomalous nanofluids did. Furthermore, a greater proportion of the anomalous nanofluids had surfactants opposed to the conventional nanofluids (41% vs. 22%).

Surfactants thermally degrade at high temperatures depending on the concentration of the surfactant and the type of surfactant used. The maximum temperature under which surfactants were employed in the data set was 40 °C,

in the study of Srinivas and Venu Vinod [39], who used cetyltrimethylammonium bromide. For this surfactant, degradation is observed at temperatures in excess of 100 °C [123], and hence the integrity of the surfactants should not be an issue in this case. Suresh et al. [32] used sodium lauryl sulphate at 30 °C. This surfactant degrades at temperatures in excess of 200 °C [124], and hence would have remained intact in the aforementioned study. All other studies that employed surfactants used milder temperatures, and hence thermal degradation can be disregarded. The same can be assumed for other cases. Thus, in this concentration range ($\phi \leq 0.2$ vol%), stable zeta potentials alone are insufficient to yield anomalous enhancement, rather the configuration of stable pH and surfactants (especially the former) increases the probability of formulating an anomalous nanofluid.

Indeed, the effect of nanofluid stability is imperative, as, for example, one-step methods have been shown to yield much more stable nanofluids with significantly greater performance than those synthesised using two-step methods [8]. Increasing nanofluid stability through increased ultrasonication has also been reported to increase the enhancement [20]. Increased stability does not guarantee increased enhancement however, as reported by Yang et al. [27], who employed surfactants and pH controllers in an Al_2O_3–water nanofluid yet observed no change in thermal conductivity. This could be attributed to their use of relatively dense nanofluids ($\phi > 0.5$ vol%), as, in contrast, Wang and Li [28] used a dilute Al_2O_3–water nanofluid ($\phi \leq 0.2$ vol%) and observed increased enhancement with increased stability. The above indicates the differing effects of nanofluid stability in the anomalous/conventional enhancement modes.

The effect of measurement techniques is considered in Fig. 10b, with the anomalous nanofluids predominantly characterised using the THW and TPS methods. Relatively few data points ($< 10\%$) arose from THWe and MZI techniques, although from Fig. 5, TPS yielded significantly greater enhancement compared to the THW(e) method. Interestingly, the use of an electrically conductive sensor was more likely to yield conventional enhancement, as opposed to the anomalous enhancement using such a device reported by Buongiorno et al. [14]. The issue of measurement error is analysed further in the next section.

Considering finally the different concentrations and nominal diameters employed in the considered nanofluids through the violin plots in Figs. 11a and b respectively, the anomalous nanofluids had on average lower concentrations and larger nominal diameters (diameters up to ≈ 140 nm were used in the anomalous nanofluids). Thus, there is indication that more dilute nanofluids facilitate the anomalous enhancement mode, whilst there is a limit to the benefit of using smaller nanoparticles. In support of the latter point, Chen et al. [31] observed a reduction in enhancement on addition of a surfactant. This could be attributed to the increase in

interfacial resistance [26, 125] and ballistic scattering [64], which are more significant for smaller particles ($d = 15$ nm in the study of Chen et al. [31], whilst Wang and Li [28] used $d = 33$ nm and observed increased enhancement with increased stability). This is also supported by further investigation of the full dataset, where for anomalous enhancement with $d \leq 15$ nm, no surfactants or pH controllers were used. Furthermore, reducing the nanoparticle size further reduced enhancement to within theoretical bounds (e.g. in the study Hemmat Esfe et al. [23], $d = 5$ nm). Indeed, Evans et al. [126] reported interfacial resistance to be significant for characteristic lengths less than 20 nm.

Thus, for the system conditions considered in the present work (ambient pressure), the findings suggest that it may be possible to formulate an Al_2O_3–water nanofluid that exhibits thermal performance akin to the anomalous enhancement mode through the use of low nanoparticle concentration ($\phi \leq 0.2$ vol%), not too small nominal diameter ($d \geq 15$ nm) and the employment of a pH controller (if not a surfactant, although this is less favourable for practical heat transfer applications, as some surfactants degrade at higher temperatures). If one uses a nanofluid with $d < 15$ nm, pH controllers/surfactants should not be used. In all cases, sufficient ultrasonication (at least 4 h, if using an ultrasonic bath [20]) should be performed.

The preceding characterisation of anomalous Al_2O_3–water nanofluids offers some further insight into the literature. For example, Keblinski et al. [91] dismissed the possibility of nanofluids exhibiting anomalous enhancement in thermal conductivity, justified by their presentation of a plethora of data demonstrating nanofluids to fall within the limits of effective medium theory (HS bounds). However, at least for Al_2O_3–water nanofluids, they had only one datapoint in the anomalous range of enhancement ($\phi = 0.02$ vol%, from [53]). Hence, if they extended the number of samples in this region of low volumetric concentration, as has been done in Fig. 4 for $\phi < 0.2$ vol%, their conclusions may have differed. Indeed, they observed such anomalous enhancement for the Fe_3O_4-water nanofluid of Zhu et al. [127]; however, this result was uncorroborated, justifying their conclusions. Another imperative work is the benchmark study of Buongiorno et al. [14], in which 30 institutions performed round robin thermal conductivity measurements on samples of identical nanofluids, concluding there to be no anomalous enhancement. Again, the presently deduced characteristics of anomalous Al_2O_3–water nanofluids can aid in understanding their result. Their Al_2O_3–water (set 1, sample 1) nanofluid was constituted of alumina nanorods with a nominal characteristic dimension of 10 nm at a concentration of 1 vol% with no surfactants or pH controller (ultrasonic dispersion only). Although their nanoparticles were not spherical, their use of nanoparticles with a concentration greater than 0.2 vol% and small characteristic size results in

Fig. 10 Bar plots (reduced dataset) of percentage of observations based on **a** stability characteristics and **b** measurement technique for anomalous/ conventional thermal conductivity enhancement modes in Al_2O_3–water nanofluids at atmospheric pressure
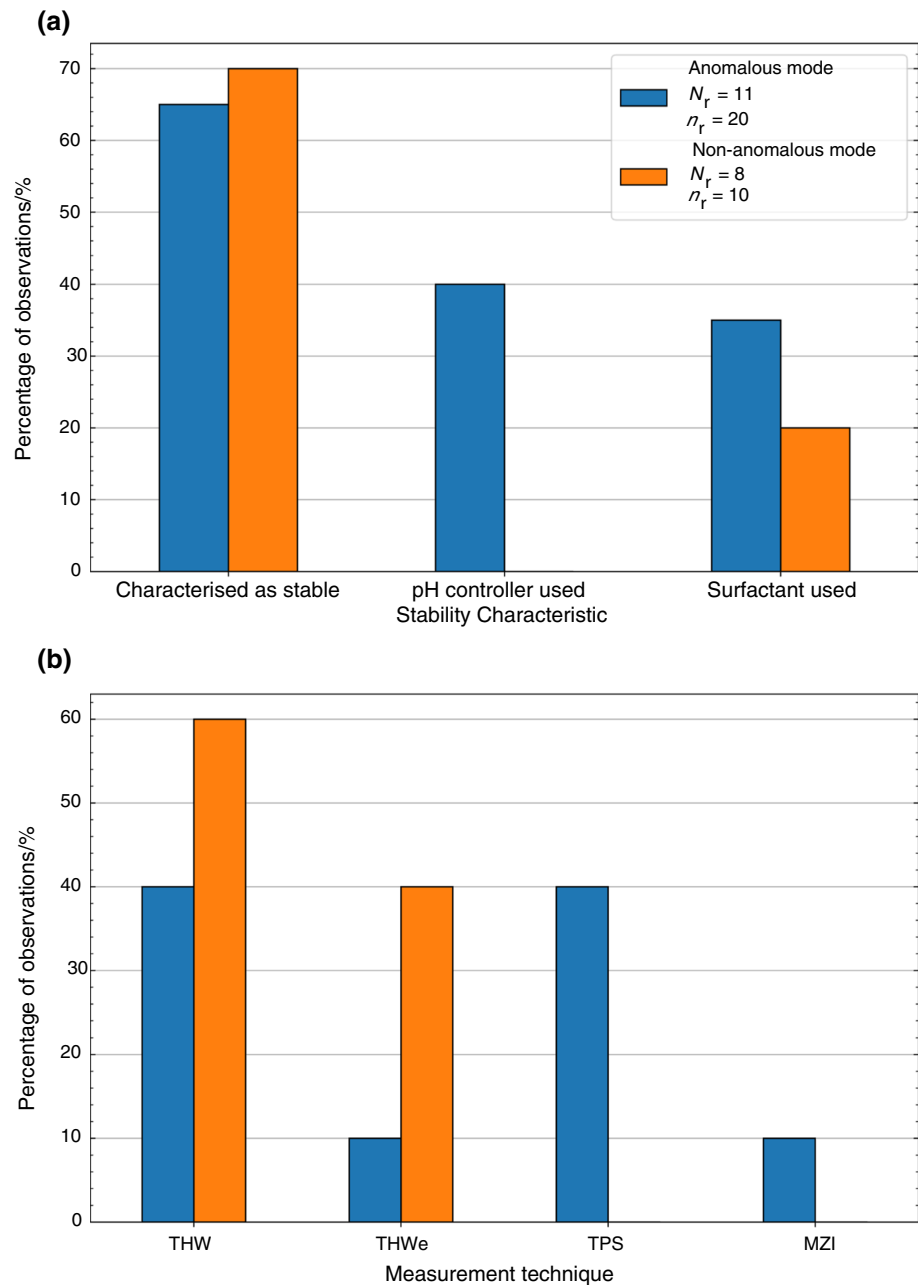
a nanofluid outside the characteristic anomalous zone ($\phi <$ 0.2 vol%, Fig. 7) and susceptible to significant interfacial resistance effects respectively ($d < 20$ nm [126]).

The preceding insights lead to two recommendations. Firstly, the characteristics of anomalous Al_2O_3–water nanofluids, identified in the present work, should be further investigated and verified, ideally by a targeted benchmark study akin to the one of Buongiorno et al. [14] (to corroborate results as has been done in the present literature analysis). Secondly, these anomalous characteristics should be deduced for other nanofluids, such as the Fe_3O_4-water nanofluid of Zhu et al. [127], and then also tested in benchmark studies.

This may require additional experimentation, as there is less available data for nanofluids other than Al_2O_3-water.

Anomalous enhancement or measurement error?

As mentioned at the end of Sect. 4.5, the supposed anomalous enhancement that has been observed—opposed to representing true physical phenomena—may simply be an artefact of measurement error. This view was supported by Antoniadis et al. [128], who concluded that most of the nanofluid thermal conductivity data, measured using the THW method, were inaccurate, since conditions for accurate THW measurements are rarely satisfied. It is noted

Fig. 11 Violin plots (reduced dataset) of **a** volumetric concentration and **b** nominal diameter distributions for anomalous/conventional thermal conductivity enhancement modes in Al_2O_3–water nanofluids at atmospheric pressure
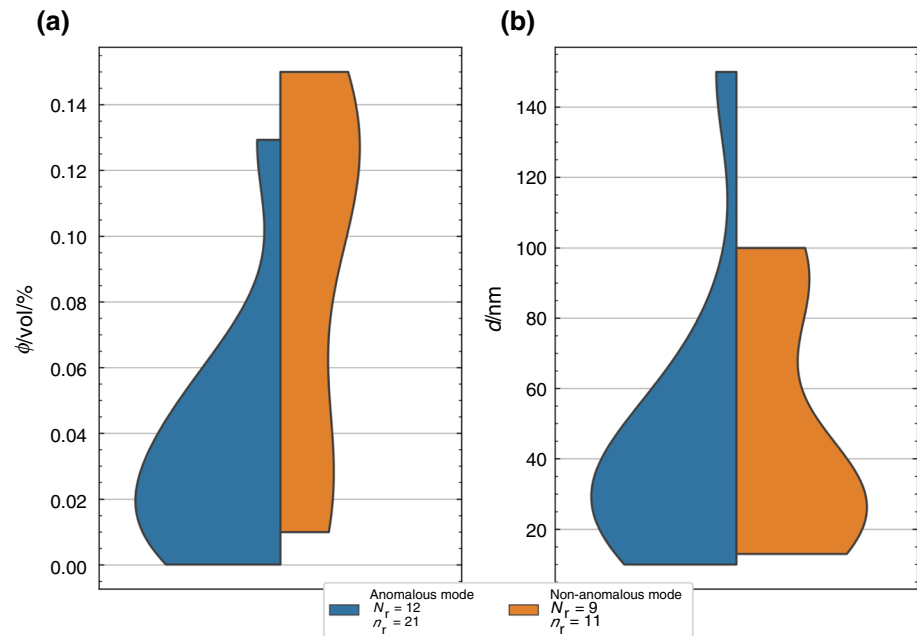
that the conditions for accurate THW measurements are (a) an electrically insulated sensor (for polar liquids such as water), (b) a thin wire (< 30 μm in diameter) to enable the line source approximation, (c) two wires to compensate for end effects, and (d) minimise convection by using low temperature rise (< 4 K) and short duration of measurement (< 1 s). Considering the most popular THW device (KD2 Pro coupled with the KS-1 sensor for liquids), the probe is coated in Teflon and is thus electrically insulated. However, it consists of only one wire and hence end effects could be significant. However, Lee et al. [47] argued that end effects can be neglected for a single wire with a length/diameter ratio larger than 4000. Computing this value for the KS2 probe yields 6 cm/0.13 cm = 46, and, thus, end effects cannot be neglected for this device. The line source approximation would also appear to be invalid, as the sensor probe is too thick, introducing axial conduction and measurement error, with increasing error for smaller aspect ratios and longer experiment times. However, according to Hammerschmidt and Sabuga [129], the conditions required to mitigate this error to a few percent are easily met when using liquids and solids. It must be stressed that this device (the KD2 Pro) is designed for geological measurements, and the application of this device to colloidal systems may have unknown uncertainties.

Tertsinidou et al. [113] conveyed a similar sentiment regarding the accuracy of nanofluid thermal conductivity measurements using the THW method, identifying several publications in which the conditions for accurate measurements were violated. Interestingly they expressed confidence in the accuracy of TPS devices (a technique used to characterise almost half of the anomalous nanofluids identified

in Fig. 7), and, when removing measurements they deemed to be unreliable, found the resulting Al_2O_3–water nanofluid thermal conductivity data to lie reasonably close to the Hamilton Crosser predictions (although they still observed several data points exceeding the predictions of this model). A similar finding was reported by Antoniadis et al. [128].

Hassleman [130] responded to the work of Tertsinidou et al. [113], investigating the validity of the THW model, positing nanoparticle collisions at the probe surface to cause a strong positive temperature dependence of the (finite) interfacial heat transfer coefficient. This hypothesis accounted for the effect of particle size, with smaller particle diameters increasing this effect and hence the augmentation of the heat transfer coefficient. Most of the preceding arguments and recommendations were largely dismissed by Assael and Wakeham [131]. For example, the temperature increase (< 4 K) is too small for the thermophysical properties of interest to vary significantly. The importance of nanoparticle collisions with the measurement probe was refuted based on an order of magnitude analysis from which it was determined that the nanoparticles would have to convey insensible amounts of heat in order to yield the observed heat transfer enhancement. This result informs on the unusual transitional behaviour from the anomalous to conventional enhancement modes observed in Fig. 4, where, for $\phi > 0.2$ vol%, a sudden drop is observed in the enhancement. One could argue that at those low concentrations (in the anomalous mode), the size of agglomerates would be reduced and nanofluid stability enhanced, possibly contributing to a net increase of the nanoparticle collisions with the probe surface (although there would be significantly fewer

nanoparticles) ultimately artificially augmenting the measured thermal conductivity.

From the preceding discussion, it is apparent that controversy remains regarding the accuracy of thermal conductivity measurements of nanofluids. Although most authors verify their thermal conductivity measurements by comparison of a pure basefluid measurement with a reference value (e.g. $\sim 0.6 \mathrm{Wm}^{-1} \mathrm{K}^{-1}$ for water under ambient conditions), it is the extension of the considered method to measuring nanofluid thermal conductivity, which is troublesome. As mentioned, the most popular commercial device (KD2 Pro), is made for geological measurements, and, although the KS-1 probe is designed for liquid thermal conductivity measurements, it has not been verified for use with nanofluids let alone any other colloidal suspensions [131].

To investigate further the effect of insulation on the THW method, measured values of thermal conductivity ratios at identical volumetric concentrations were compared, based on whether an insulated sensor was employed in the THW technique, and the results are shown in Fig. 12. The effect of temperature was eliminated by considering only those data points which fell within ambient values. The vertical lines on the bars represent the distribution of the variable, in which case the bar height represents the average. This distribution in thermal conductivity ratio for the same volumetric concentration in Fig. 12a was caused in part by the differing nominal diameters used, as can be seen in Fig. 12b. In agreement with Fig. 5, THW measurements yield greater enhancement on average (in fact, consistently, at least for these data points) than those without electrically insulated sensors (THWe). It is important to emphasise that in Fig. 12 the effect of differing concentrations and temperature has been fully removed, indicating that either the measurement technique, different nominal diameters or stability characteristics are the cause for the variation in the measured thermal conductivities. Assuming the effect of the measurement technique was negligible, one would expect the greater enhancement observed by the THW method to correspond to smaller nominal particle diameters, but as can be seen in Fig. 12b, this is not the case (the THW cases used either larger or similarly sized nanoparticles). The case of $\phi = 0.5$ vol% is an exception, as the nominal diameter of the THWe data was less than 20 nm, and hence may suffer from significant interfacial resistance, thus explaining the lower recorded enhancement. Although conversely, one could argue the reduction in nanoparticle diameter and thus increase in surface area should cause some enhancement in heat transfer [132]. For example, Xie et al. [51] observed thermal conductivity enhancement to increase monotonically with specific surface area (for a fixed nanofluid concentration), and to then decrease after a critical value (possibly due to the increased contribution of interfacial resistance).

Overall, the suggestion that the use of an electrically conductive sensor could artificially enhance the measured thermal conductivity—leading to false reports of anomalous enhancement—is discredited by the present results. On the contrary, the evidence suggests that the use of an electrically insulated sensor yields greater measured enhancements than methods with an uninsulated sensor. However, the possibility remains for this discrepancy to be attributed to other factors such as particle size distribution, stability, particle shape and experimental procedure (i.e. time between preparation of formulation and measurement). Further, the sample sizes for these comparisons are quite small (15 publications), and hence statistically strong conclusions cannot be drawn.

A further indication of measurement technique reliability is offered by the benchmark study of Buongiorno et al. [14], where, although deviations up to $\pm 5\%$ were reported for absolute measured values of nanofluid/basefluid thermal conductivity for Al_2O_3–water nanofluids, these discrepancies were systematic and, thus, eliminated when the effective nanofluid thermal conductivity (i.e. enhancement) was computed.

Finally, by simple reasoning, if conventional enhancement was reported for nanofluids denser than 0.2vol%, i.e. 'reliable' measurements were obtained for these concentrations, what possible physical mechanism could cause the same measurement techniques to be insensible for more dilute nanofluids, in which there are significantly fewer nanoparticles present in the system? On the contrary, it is more likely that the change in system condition (lower concentration and particle number density), results in some novel system configuration operating on some—as of currently—unknown mechanism(s) of heat transfer enhancement. The issue of measurement error is further mitigated by the employment of a mixture of measurement techniques, including the TPS method, which has been stated to be accurate [113].

Thus, from the preceding discussion, the possibility of anomalous enhancement in nanofluid thermal conductivity arising due to a real physical phenomenon opposed to artificial measurement errors remains open.

Anomalous mechanism(s)

The possibility of the anomalous thermal conductivity enhancement observed in Fig. 7 to be attributed wholly to measurement error has been somewhat refuted in the previous section, thus providing some evidence to indicate the possible existence of physical mechanism(s) that lead to the anomalous behaviour. As explained in the Results section, several hypothetical mechanisms have been proposed in the literature over the last few decades, which aim to account for the anomalous thermal conductivity enhancement observed
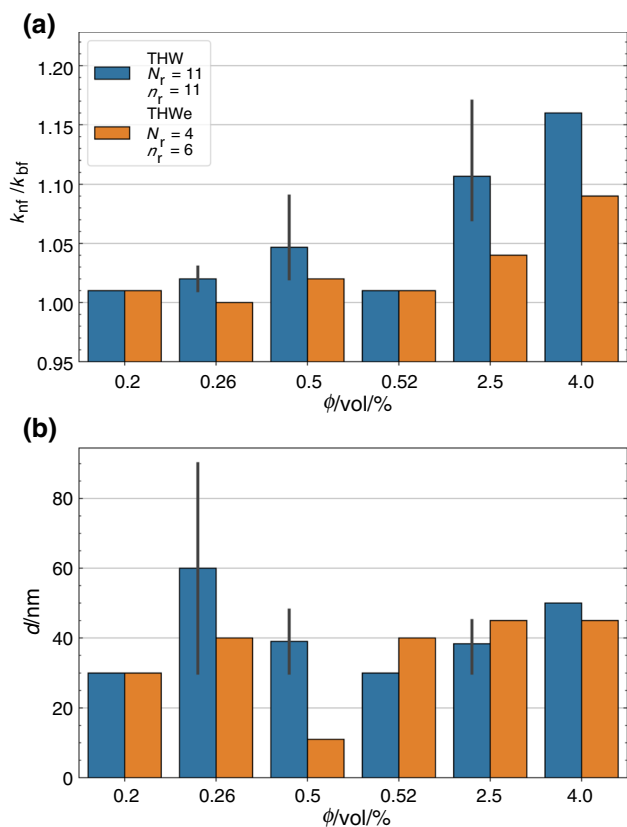
(a)

(b)

Fig. 12 Bar plots (reduced dataset) of **a** thermal conductivity ratio and **b** nominal diameter versus volumetric concentration for insulated/non-insulated transient hot-wire methods (293 K < T < 300 K)

in nanofluids by extending EMT (Maxwell's equation [15]) to account for the postulated mechanism(s).

The key possible mechanisms considered in the current section are the formation of chain-like structures by the dispersed phase, Brownian motion effects (induced nanoconvection) and surface effects (Kapitza resistance, the formation of a nano-layer and thermophoresis). Some of these mechanisms can be tested, such as chain-like structures, which have been observed via SEM [21]. Conversely, it is difficult to probe the miniature length-scale of the nano-layer, which is hence chiefly investigated using MDS approaches.

Chain-like structures

The formation of percolating chain-like structures has been observed experimentally for Al_2O_3–water nanofluids with $\phi < 0.015$ vol% (stable pH and zeta potential values) [21]. From Fig. 7, anomalous enhancement was observed for nanofluids up to 10 times denser than this concentration (concentrations up to 0.2 vol%). The formation of such chain-like structures can only yield enhancement that does not exceed the limit of the HS upper bound whilst,

in addition, the enhancement due to chain-like structures should decrease both at smaller nanofluid concentrations as there are insufficient nanoparticles present in the system to form them [8]. Compounding these factors, the formation of chain-like structures alone does not seem to explain the reported anomalous enhancement.

Moreover, the HS upper bound should be reduced at these low concentrations to account for the diminished effects of chain-like structures compared to the dominant dispersed phase conduction paths that are established at higher concentrations, possibly encapsulating additional nanofluids in the anomalous zone [8]. Such a model was formulated by Buongiorno et al. [14].

Brownian motion and induced nanoconvection

Another popular proposed mechanism is Brownian motion of the nanoparticles, which may induce additional convection of the surrounding fluid (Brownian motion induced nanoconvection). It is generally accepted that the Brownian motion of the nanoparticles is insignificant compared to the thermal diffusivity of the basefluid. However, the induced nanoconvection remains a point of contention [8, 91, 133].

Azizian et al. [134] theoretically compared the timescales of Brownian motion, nanoconvection and thermal diffusion for a nanofluid comprised of 5 nm nanoparticles, finding that the timescales of nanoconvection and thermal diffusion were similar (10^{-11} s, as compared to 10^{-8} s for Brownian motion). This suggests that the contribution of nanoconvection to nanofluid thermal conductivity cannot be neglected. These findings were also corroborated by Prasher et al. [103], who performed an order or magnitude analysis. Pang et. al. [135] reported dynamic mechanisms (including nanoconvection) to contribute almost 90% of the thermal conductivity enhancement observed in nanofluids.

Azizian et al. [136] experimentally investigated alumina and titania nanofluids, using large enough particle sizes (70 and 30 nm respectively) such that ballistic transport did not occur in the particles and large agglomerates did not form (they noted larger agglomerates formed with smaller particle sizes). Hence, this enabled them to isolate the effects of nanoconvection. They tested various theoretical models against their data and found the semi-empirical model of Chon et al. [58] best predicted their results. This model accounts for nanoconvection and was derived from alumina nanofluid experimental data. Interestingly, Azizian et al. [136] found this model to also accurately predict the thermal conductivity of their titania nanofluid. They found the agreement between their data and the model to vary depending on the dominance of nanoconvection, which they stated to become more significant for smaller particle sizes and higher concentrations. Overall, nanoconvection is seen to

be a significant mechanism in augmenting heat transfer in nanofluids.

Surface effects

There are three major surface effects to consider, Kapitza resistance (due to phonon scattering at interfaces [137]), the formation of a nano-layer on the surface of the particle (with an intermediate thermal conductivity between that of the particle and the basefluid), and thermophoresis (a driver of mass flux due to a temperature gradient, enacted by interfacial stresses—in the form of temperature inhomogeneities [138]).

The physical understanding of the Kapitza resistance is important when considering the results of the theoretical modelling in Sect. 4.5, as the model of Jang and Choi [101]—which incorporated the effects of Kapitza resistance—was deemed the most accurate for the considered anomalous nanofluids. This appears promising; however it is most likely to be a statistical anomaly, as a non-physical value of the parameter β (relating to the ratio between effective nanoparticle conductivity—which should be reduced due to interfacial resistance—to that of the nanoparticle alone) was obtained, viz. $\beta \sim 3$ when β should be smaller than 1 by definition.

Moving on to consider studies supporting the formation of a nano-layer, Liu et al. [139] reported the hydrogen environment to be modified on addition of Al_2O_3 to glycerol, indicating the formation of hydrogen bonds, which would thus lead to the formation of an electrical double layer in polar liquids such as water [137]. The experimental works of Turanov and Tolmachev [140] and Gerardi et al. [141] found the diffusivity of water to be reduced proportionally with increasing nanoparticle concentration, indicating the inhibition of the basefluid molecules at the solid–liquid interface. The thickness of this type of nano-layer is estimated to be 5 atomic layers according to Gerardi et al. [141]. Regarding the enhancement of heat transport within the nano-layer, interfacial thermal conductance was measured experimentally by Ge et al. [142], finding hydrophilic surfaces to have interfacial thermal conductivities approximately 2–3 times greater than hydrophobic ones, attributed to the solid–liquid layering of water.

Conversely, Milanese et al. [143] performed a MDS study on Cu/CuO nanofluids, concluding surface layering to be significant for pure metals and not oxides (such as the presently considered Al_2O_3). According to Muraleedharan et al. [144], the thermal conductivity enhancement reported in MDS studies is an error caused using periodic boundaries with single nanoparticles. Instead, when multiple particles are considered, the error and associated enhancement are resolved. Although a nano-layer of 2–3 atomic thicknesses was observed, the density changes were not expected to be

significant, and the associated enhancement deemed insufficient (nano-layer thermal conductivity ~ 1.6 times greater than the basefluid thermal conductivity) to yield significant enhancement. Keblinski et al. [91] argued that enhancement due to nano-layering would be significant only for exceptionally small nanoparticles (< 0.01 nm).

In addition, from Fig. 9, the nano-layer model of Xue and Xu [98] was found to be quite inaccurate for the anomalous nanofluids. Different values of nano-layer thermal conductivity were tested in this model (up to the nanoparticle thermal conductivity), yielding no significant increases in accuracy. In fact, Liang and Tsai [145], reported the thermal conductivity of the nano-layer to be ~ 2 times greater than the basefluid thermal conductivity in a MDS study, hence the value of k_1 assumed in Table 3 for the Xue and Xu model [98] was already sensible.

Touching finally on thermophoresis, although well understood in gases, understanding of this phenomenon in liquids (and colloidal suspensions) is much more limited in comparison [138, 146, 147]. Thermophoresis in colloids is a manifestation of a larger spectrum of phoretic processes, driven by interfacial stresses (hence thermophoresis is not observed in pure liquids, nor in dense colloidal suspensions, even in the presence of a temperature gradient), with these interfacial stresses induced by variations in composition, pH and temperature [138]. Thermophoresis is an interface dominated phenomenon [146], so that, when interfacial conditions are normalised (i.e. surface charge), thermophoretic mobility has been reported to become insensitive to particle size [147], which is an interesting characteristic since a lot of attention is given to the influence of nanoparticle size on nanofluid heat transfer. Although difficulties have been faced in isolating thermophoresis from the other phoretic processes in colloids, novel experimental techniques have been developed and employed to probe this interesting phenomenon (in colloidal suspensions constituted of polymers). These demonstrated the significant effects of parameters such as pH and the employment of surfactants on thermophoretic mobility [138]—with similar effects expected for the presently considered metallic nanoparticles. However, the extent to which these experimental results can be trusted is difficult to evaluate, at least when pertaining to thermophoresis, as modifying the surface charge of a colloid will affect the other phoretic processes, such as electrophoresis (thermophoresis depends only on temperature inhomogeneities). This difficulty in isolating the thermophoretic effect is further compounded by impurities. Further, uncertainties up to 50% have been reported in experimental studies investigating thermophoresis in nanofluids [148, 149].

With thermophoresis introduced, it is interesting to return to the concept of Kapitza resistance somehow enhancing heat transport. Thermophoresis is driven by inhomogeneities in temperature at the particle–fluid interface [147]. Although

most theoretical models of nanofluid thermal conductivity neglect the effect of temperature inhomogeneities within/at the surface of a nanoparticle, the rotational and translational mobility of a nanoparticle has been posited to cause such non-equilibrium effects, which then drive the thermophoretic process (see the MDS study of Sergis and Hardalupas [150]). From this, although Kapitza resistance is normally attributed as a detriment to heat transport, there may exist a condition in which the augmented temperature inhomogeneities (mismatch) brought about by Kapitza resistance could enhance the thermophoretic mobility of nanoparticles such that overall, an enhancement in thermal conductivity is observed.

The preceding discussion on surface effects, and their posited impact on mechanisms such as thermophoresis, ultimately determining the alteration in the thermal conductivity of nanofluids, is further supported by the present results. For example, no conventional nanofluids had their pH controlled (from Fig. 10a) and the use of surfactants was more likely to yield an anomalous nanofluid than not. Both methods enhance stability, but in different ways. Surfactants are constituted of a hydrophilic 'head' and hydrophobic 'tail', where in the present context, the tail would adsorb to the nanoparticle surface [151]. This enhances stability by screening the VdW forces between nanoparticles, preventing agglomeration, and is classed as steric stabilisation [152]. On the other hand, the employment of pH control is known as electrostatic stabilisation and involves the formation of a surface charge through various mechanisms, resulting in the formation of a "tightly bound" electrical double layer [152], effectively introducing a repulsive electric force between the nanoparticles [137]. Surfactants yield greater stability (i.e. agglomeration resistance), although the thickness of this surfactant layer is expected to inhibit heat transfer [152], especially when compared to the dense electrical double layer. Overall, it appears that there is an unknown mechanism related to the pH control, which leads to favourable conditions for enhancement through the interplay of the above-mentioned surface effects.

Conclusions

The present study critically assessed literature reports of anomalous thermal conductivity enhancement in alumina–water nanofluids. To do this, data pertaining to the experimentally measured thermal conductivity enhancement of (spherical) Al_2O_3–water nanofluids under ambient pressure was collated from 72 independent, high-quality publications. Key parameters such as volumetric nanoparticle concentration, nominal (manufacturer stated) nanoparticle diameter and suspension stability criteria were also recorded. After randomly sampling data points to remove

bias, an extensive statistical analysis and assessment was conducted, yielding the following key conclusions:

(1) Anomalous enhancement in nanofluid thermal conductivity was observed in 17% of the collected samples, yielding the following characteristics and recommendations.

    (a) Observed for $\phi < 0.2$ vol% (conventional enhancement in this region was also reported, although at a relatively rare frequency).

    (b) These 'anomalous' nanofluids were predominantly stabilised via pH control (in the same volumetric concentration regime, no conventional nanofluids were pH controlled).

    (c) When using small nanoparticles ($d < 15$ nm), pH controllers and surfactants should not be used to achieve anomalous enhancement (doing so may reduce the effective agglomerate size, yielding significant interfacial resistance which is the case for $d < 15 - 20$ nm).

    (d) In all cases, sufficient ultrasonication should be used. In ultrasonic bath applications, this is typically at least 4 h. Where an ultrasonic probe is used, the applied power should be minimised and the nanofluid ultrasonicated to the point prior to reaggregation.

    (e) On the employment of a selection of theoretical and semi-empirical thermal conductivity models provided in the literature, some models were only superficially accurate, due to their extensive basis on non-linear equations with statistically fitted coefficients. Omitting these, the (Brownian motion induced) nanoconvection model of Jang and Choi [101] was the most accurate and physically sensible, yielding similar accuracy for both anomalous and conventional nanofluids (standard error 5–10%). It had two linear proportionality constants, only one of which had a theoretical basis, β (defined as the ratio of the effective nanoparticle conductivity, including the effect of interfacial resistance, to the thermal conductivity of the nanoparticle alone). For the conventional nanofluids, a reasonable value was obtained ($\beta \sim 0.01$), whereas for the anomalous nanofluids, the process of statistical fitting yielded a non-physical value ($\beta \sim 3$). From further analysis, this non-physical value was determined to represent a statistical anomaly opposed to an indicator of some physical mechanism, although it was concluded that possible enhancement from surface effects should not be neglected.

(f)   The remaining variation in the data was attributed to a combination of a gap in the theoretical understanding, additional unaccounted factors of importance (e.g. suspension stability, particle size distribution, time between suspension formulation and measurement) and, potentially errors caused by the employed underlying measurement techniques.

(2)   Although several opposing views have been expressed regarding the reliability of the underlying thermal conductivity measurement techniques when applied to nanofluids, there is no conclusive evidence yet to prove that the observed enhancement is caused by measurement error.

(a)   From the literature it is seen that sensible and reliable thermal conductivity measurements are achieved for alumina–water nanofluids denser than 0.2 vol%. The fact that there is an abrupt change in the thermal behaviour of alumina nanofluids at this concentration is incredibly strange. Given that this behaviour is concentration dependent, regardless of measurement technique, suggests that the particle size distribution of the nanofluid and stabilisation method are responsible for this step change.

(b)   It may be that at concentrations lower than the critical concentration for alumina–water nanofluids (0.2 vol%), the reduced particle number density allows for a lower effective particle size of the dispersed media. These smaller agglomerates and populations of individual nanoparticles will exhibit greater Brownian motion velocities, enhancing heat transport. In addition to this, the nanoconvection induced in the wake of the augmented motion of the dispersed phase will also be enhanced, further increasing thermal heat transport. It should be noted that of the considered theoretical models in the present paper, the nanoconvection models proved to be most accurate—providing some evidence to support the contribution of this mechanism. A cut-off concentration for the formation of chain-like structures has been reported in the literature [21]. These chains form highly efficient fractal structures that also contribute to thermal transport enhancement.

(c)   The issue of measurement error in the observations of anomalous enhancement is further mitigated by the employment of a mixture of measurement techniques, including the TPS method, which has been stated to be accurate [113].

(d)   The widely believed hypothesis that parasitic electrical currents augment the enhancement reported by electrically conductive THW probes (for example, reported by Buongiorno et al. [14]) is contradicted by the present study, with evidence to suggest the contrary (although the statistical power of this finding is weak, as the sample size was small, $n = 15$).

(e)   The observed anomalous enhancement data points exceeded the experimental uncertainty ($> 10\%$ enhancement versus $\pm 5\%$ maximal uncertainty [113]). This issue is further refuted by the elimination of systematic measurement error on computation of the effective thermal conductivity (i.e. enhancement), as reported by the benchmark study of Buongiorno et al. [14], who performed 30 independent measurements of an identical Al_2O_3–water nanofluid.

The novelty of the current work lies in analysing the conditions under which anomalous thermal conductivity enhancement has been observed for alumina–water nanofluids. Common conditions exhibiting anomalous effects have been discovered. The anomalies are observed in nanofluids with low nanoparticle concentrations ($\phi \leq 0.2 vol\%$) and in those making use of electrostatic stabilisation (through pH control) as opposed to steric stabilisation (using surfactants) as the suspension control method. Additionally, where small particle sizes were employed ($d < 15$ nm), no surfactant or pH control should be employed to prevent significant interfacial resistance. These shared characteristics amongst the reported anomalous observations indicate that the underlying physical mechanisms of heat transfer involved are affected by nanofluid preparation and should be further investigated. Quantifying these conditions also enables the refutation of replication studies claiming to disprove the existence of anomalous enhancement, as these studies did not employ the same conditions (e.g., steric/no stabilisation, particle sizes too small—leading to significant interfacial resistance, concentrations too large).

With these outcomes in mind, the following recommendations are made for future work:

(1)   The contention over measurement error can be resolved through future work employing THW measurement apparatus that satisfies the requirements outlined by Antoniadis et al. [128] to investigate the anomalous parameter space of interest for alumina–water nanofluids ($\phi < 0.2$ vol%, electrostatic stabilisation).

(a)   If the anomaly is reliably and repeatably demonstrated then this supports and justifies further

investigation into the underlying theory of heat transfer in such fluids.

(b) Expansion of the work to other nanoparticle materials could yield additional insight into the thermal conductivity enhancement (something that could not be done in the current study due to the small number of publications that would have yielded a statistically insignificant sample size).

(2) Given the difficulty in achieving replication in previous benchmark studies [14], it is recommended that the nanofluid research community endeavours on establishing a standard protocol of nanofluid manufacturing, experimentation and measurement.

(a) This protocol would standardise important factors such as the deposited ultrasonic energy per unit mass in the nanofluid and the time between dispersion and the onset of thermal conductivity measurement.

(b) The stability and thermal performance of nanofluids are intrinsically linked to these parameters, and some may be more important than others—hence a parametric analysis process is required.

(3) Once these conditions have been satisfied, the presently characterised anomalous alumina–water nanofluids should be investigated in a collaborative benchmark study (akin to that of Buongornio et al. [14]). If successfully validated, the contention over the contribution of measurement error can be dispelled.

(4) Following this stage, further work should proceed on investigating the fundamental physical mechanisms giving rise to the anomalies observed.

(a) The research can extend to other materials and basefluid combinations, which may potentially yield additional benefits (such as more favourable breakup mechanisms [12]).

(5) With the augmentative thermal behaviour of nanofluids understood, research efforts should shift to best realising the requirements needed for commercial development. These requirements are different to those concerning research outcomes in a very well controlled laboratory environment.

Author contribution All authors contributed to the study conception and design. Material preparation, data collection and analysis were performed by Mustafa Iqbal. The first draft of the manuscript was written by Mustafa Iqbal and all authors commented on previous versions of the manuscript. All authors read and approved the final manuscript.

Declarations

References

1. Hashimoto S, Yamaguchi S, Harada M, Nakajima K, Kikuchi T, Ohishi K. Anomalous behavior of liquid molecules near solid nanoparticles: novel interpretation on thermal conductivity enhancement in nanofluids. J Colloid Interf Sci. 2023;638:475–86.

2. Hashimoto S, Kurazono K, Yamauchi T. Anomalous enhancement of convective heat transfer with dispersed SiO_2 particles in ethylene glycol/water nanofluid. Int J Heat Mass Transf. 2020;150:119302.

3. Somarathna C, Samaraweera N, Jayasekara S, Perera K. A molecular dynamics study of thermal conductivity and viscosity in colloidal suspensions: from well-dispersed nanoparticles to nanoparticle aggregates. Appl Therm Eng. 2023;229:120651.

4. Woo WK, Hung YM, Wang X. Anomalously enhanced thermal conductivity of graphite-oxide nanofluids synthesized via liquid-phase pulsed laser ablation. Case Stud Thermal Eng. 2021;25:100993.

5. Vinod S, Philip J. Thermal and rheological properties of magnetic nanofluids: recent advances and future directions. Adv Colloid Interface Sci. 2022;8:102729.

6. Sridhara V, Satapathy LN. Al_2O_3-based nanofluids: a review. Nanoscale Res Lett. 2011;6:456.

7. Haddad Z, Oztop HF, Abu-Nada E, Mataoui A. A review on natural convective heat transfer of nanofluids. Renew Sustain Energy Rev. 2012;16:5363–78.

8. Lee J-H, Lee S-H, Choi C, Jang S, Choi S. A review of thermal conductivity data, mechanisms and models for nanofluids. Int J Micronano Scale Transp. 2010;1:269–322.

9. Sergis A, Hardalupas Y. Anomalous heat transfer modes of nanofluids: a review based on statistical analysis. Nanoscale Res Lett. 2011;6:391. https://doi.org/10.1186/1556-276X-6-391?site=nanoscalereslett.springeropen.com.

10. Khurana D, Choudhary R, Subudhi S. A critical review of forced convection heat transfer and pressure drop of Al_2O_3, TiO_2 and CuO nanofluids. Heat and Mass Transf. 2017;53:343–61.

11. Kumar PM, Kumar J, Tamilarasan R, Sendhilnathan S, Suresh S. Review on nanofluids theoretical thermal conductivity models. Eng J. 2015;19:67–83.

12. Iqbal M, Sergis A, Hardalupas Y. Stability of nanofluids fundamentals and transport properties of nanofluids. Royal Soc Chem. 2022;2022:41–70.

13. Kouloulias K, Sergis A, Hardalupas Y (2016) The influence of nanofluid pH on natural convection. In: 12th international conference on heat transfer, fluid mechanics and thermodynamics. pp 1465–72

14. Buongiorno J, Venerus DC, Prabhat N, McKrell T, Townsend J, Christianson R, et al. A benchmark study on the thermal conductivity of nanofluids. J Appl Phys. 2009;106:094312. https://doi.org/10.1063/1.3245330.

15. Maxwell JC. A treatise on electricity and magnetism. Oxford: Clarendon Press; 1881.

16. Teng T-P. Thermal conductivity and phase-change properties of aqueous alumina nanofluid. Energy Convers Manag. 2013;67:369–75. https://doi.org/10.1016/j.enconman.2012.12.004.

17. Moldoveanu GM, Huminic G, Minea AA, Huminic A. Experimental study on thermal conductivity of stabilized Al_2O_3 and SiO_2 nanofluids and their hybrid. Int J Heat Mass Transf. 2018;127:450–7.

18. Iacobazzi F, Milanese M, Colangelo G, Lomascolo M, de Risi A. An explanation of the Al_2O_3 nanofluid thermal conductivity based on the phonon theory of liquid. Energy. 2016;116:786–94.

19. Balaji V, Arulprakasajothi M, Logesh K, Tharunpillai B. Assessment of heat transfer behavior of water based alumina nanofluid. Mater Today Proc. 2018;5:20641–6.

20. Mahbubul IM, Shahrul IM, Khaleduzzaman SS, Saidur R, Amalina MA, Turgut A. Experimental investigation on effect of ultrasonication duration on colloidal dispersion and thermophysical properties of alumina–water nanofluid. Int J Heat Mass Transf. 2015;88:73–81. https://doi.org/10.1016/j.ijheatmasstransfer.2015.04.048.

21. Nimdeo YM, Srivastava A. Understanding the temperature dependence of thermo-physical properties of nanofluid suspensions using non-intrusive dynamic measurements. Exp Therm Fluid Sci. 2018;94:109–21.

22. Kundan L, Mallick SS, Pal B. An investigation into the effect of nanoclusters growth on perikinetic heat conduction mechanism in an oxide based nanofluid. Powder Technol. 2017;311:273–86.

23. Hemmat Esfe M, Saedodin S, Mahian O, Wongwises S. Thermal conductivity of Al_2O_3/water nanofluids. J Therm Anal Calorim. 2014;117:675–81.

24. Vakilinejad A, Aroon MA, Al-Abri M, Bahmanyar H, Myint MTZ, Vakili-Nezhaad GR. Experimental and theoretical investigation of thermal conductivity of some water-based nanofluids. Chem Eng Commun. 2018;205:610–23.

25. Sadeghi R, Etemad SGh, Keshavarzi E, Haghshenasfard M. Investigation of alumina nanofluid stability by UV–vis spectrum. Microfluid Nanofluidics. 2015;18:1023–30.

26. Kazemi-Beydokhti A, Heris SZ, Moghadam N, Shariati-Niasar M, Hamidi AA. Experimental investigation of parameters affecting nanofluid effective thermal conductivity. Chem Eng Commun. 2014;201:593–611. https://doi.org/10.1080/00986445.2013.782291?needAccess=true.

27. Yang Y, Oztekin A, Neti S, Mohapatra S. Particle agglomeration and properties of nanofluids. J Nanoparticle Res. 2012;14:852.

28. Xian-Ju W, Xin-Fang L. Influence of pH on nanofluids' viscosity and thermal conductivity. Chin Phys Lett. 2009. https://doi.org/10.1088/0256-307X/26/5/056601/pdf.

29. Feng X, Johnson DW. Characterization of dispersed and aggregated Al_2O_3 morphologies for predicting nanofluid thermal conductivities. J Nanoparticle Res. 2013;15:1718.

30. Haghighi EB, Nikkam N, Saleemi M, Behi M, Mirmohammadi SA, Poth H, et al. Shelf stability of nanofluids and its effect on thermal conductivity and viscosity. Meas Sci Technol. 2013;24:105301. https://doi.org/10.1088/0957-0233/24/10/105301/pdf.

31. Chen TY, Cho HP, Jwo CS, Jeng LY. Performance analysis of Al_2O_3/water nanofluid with cationic chitosan dispersant. Adv Mater Sci Eng. 2013;2013:1–8.

32. Suresh S, Venkitaraj K, Selvakumar P, Chandrasekar M. Synthesis of Al_2O_3–Cu/water hybrid nanofluids using two step method and its thermo physical properties. Colloids Surf A Physicochem Eng Asp. 2011;388:41–8.

33. Pryazhnikov MI, Minakov AV, Rudyak VY, Guzei DV. Thermal conductivity measurements of nanofluids. Int J Heat Mass Transf. 2017;104:1275–82.

34. Gharagozloo PE, Eaton JK, Goodson KE. Diffusion, aggregation, and the thermal conductivity of nanofluids. Appl Phys Lett. 2008;93:103110.

35. Kim S, Tserengombo B, Choi S-H, Noh J, Huh S, Choi B, et al. Experimental investigation of heat transfer coefficient with Al_2O_3 nanofluid in small diameter tubes. Appl Therm Eng. 2019;146:346–55.

36. Shinde SM, Patil PA, Bhojwani VK. An experimental study to investigate the dynamic behaviour of thermal conductivity for different concentrations of Al_2O_3 nanofluid. Int J Amb Energy. 2018;2018:1–6.

37. Alias H, Ani MFC, Saad SF, Ngadi N. Heat transfer of alumina-deionized water nanofluids in concentric tube heat exchanger. AIP Conf Proc. 2017;2017:020001. https://doi.org/10.1063/1.5010438.

38. Wang R-T, Wang W-C. Alumina NAE comparisons to various neutral aqueous solutions inside battery. J Mech. 2016;32:369–79. https://doi.org/10.1017/jmech.2015.86.

39. Srinivas T, Venu VA. The effective thermal conductivity of water based nanofluids at different temperatures. J Test Eval. 2016;44:20140537.

40. Lee J-H, Lee S-H, Pil JS. Do temperature and nanoparticle size affect the thermal conductivity of alumina nanofluids? Appl Phys Lett. 2014;104:161908.

41. Said Z, Sajid MH, Alim MA, Saidur R, Rahim NA. Experimental investigation of the thermophysical properties of AL_2O_3-nanofluid and its effect on a flat plate solar collector. Int Commun Heat Mass Transf. 2013;48:99–107. https://doi.org/10.1016/j.icheatmasstransfer.2013.09.005.

42. Hung Y-H, Teng T-P, Teng T-C, Chen J-H. Assessment of heat dissipation performance for nanofluid. Appl Therm Eng. 2012;32:132–40.

43. Teng T-P, Hung Y-H, Teng T-C, Mo H-E, Hsu H-G. The effect of alumina/water nanofluid particle size on thermal conductivity. Appl Therm Eng. 2010;30:2213–8.

44. Gowda R, Sun H, Wang P, Charmchi M, Gao F, Gu Z, et al. Effects of particle surface charge, species, concentration, and dispersion method on the thermal conductivity of nanofluids. Adv Mech Eng. 2010;2:807610. https://doi.org/10.1155/2010/807610.

45. Oh D-W, Jain A, Eaton JK, Goodson KE, Lee JS. Thermal conductivity measurement and sedimentation detection of aluminum oxide nanofluids by using the 3ω method. Int J Heat Fluid Flow. 2008;29:1456–61.

46. Zhu D, Li X, Wang N, Wang X, Gao J, Li H. Dispersion behavior and thermal conductivity characteristics of Al_2O_3–H_2O nanofluids. Curr Appl Phys. 2009;9:131–9.

47. Lee J-H, Hwang KS, Jang SP, Lee BH, Kim JH, Choi SUS, et al. Effective viscosities and thermal conductivities of aqueous nanofluids containing low volume concentrations of Al_2O_3 nanoparticles. Int J Heat Mass Transf. 2008;51:2651–6.

48. Masuda H, Ebata A, Teramae K, Hishinuma N. Alteration of thermal conductivity and viscosity of liquid by dispersing ultra-fine particles. Dispersion of Al_2O_3, SiO_2 and TiO_2 ultra-fine particles. Netsu Bussei. 1993;7:227–33.

49. Lee S, Choi SU-S, Li S, Eastman JA. Measuring thermal conductivity of fluids containing oxide nanoparticles. J Heat Transfer. 1999;121:280.

50. Wang X, Xu X, Choi SU. Thermal conductivity of nanoparticle - fluid mixture. J Thermophys Heat Trans. 1999;13(4):474–80.

51. Xie H, Wang J, Xi T, Liu Y, Ai F, Wu Q. Thermal conductivity enhancement of suspensions containing nanosized alumina particles. J Appl Phys. 2002;91:4568–72.

52. Das SK, Putra N, Thiesen P, Roetzel W. Temperature dependence of thermal conductivity enhancement for nanofluids. J Heat Transfer. 2003;125:567.

53. Wen D, Ding Y. Experimental investigation into convective heat transfer of nanofluids at the entrance region under laminar flow conditions. Int J Heat Mass Transf. 2004;47:5181–8.

54. Li CH, Peterson GP. Experimental investigation of temperature and volume fraction variations on the effective thermal conductivity of nanoparticle suspensions (nanofluids). J Appl Phys. 2006;99:084314.

55. Yoo D-H, Hong KS, Yang H-S. Study of thermal conductivity of nanofluids for the application of heat transfer fluids. Thermochim Acta. 2007;455:66–9.

56. Timofeeva EV, Gavrilov AN, McCloskey JM, Tolmachev YV, Sprunt S, Lopatina LM, et al. Thermal conductivity and particle agglomeration in alumina nanofluids: experiment and theory. Phys Rev E. 2007;76:061203. https://doi.org/10.1103/PhysRevE.76.061203.

57. Murshed SMS, Leong KC, Yang C. Investigations of thermal conductivity and viscosity of nanofluids. Int J Thermal Sci. 2008;47:560–8.

58. Chon CH, Kihm KD. Thermal conductivity enhancement of nanofluids by Brownian motion. J Heat Transfer. 2005;127:810.

59. Jang SP, Hwang KS, Lee JH, Kim JH, Lee BH, Choi SUS (2007) Effective thermal conductivities and viscosities of water-based nanofluids containing Al2O3 with low concentration. In: 2007 7th IEEE international conference on nanotechnology - IEEE-NANO 2007, Proceedings IEEE, p 1011–4. Available from: http://ieeexplore.ieee.org/document/4601354/

60. Williams W, Buongiorno J, Hu L-W. Experimental investigation of turbulent convective heat transfer and pressure loss of alumina/water and zirconia/water nanoparticle colloids (Nanofluids) in horizontal tubes. J Heat Transfer. 2008;130:042412.

61. Hwang KS, Ha HJ, Lee SH, Kim HJ, Jang SP, Lim HM, et al. (2009) Flow and convective heat transfer characteristics of nanofluids with various shapes of alumina nanoparticles. In: ASME 2009 Second international conference on micro/nanoscale heat and mass transfer, Vol 1. p 455–60. Available from: http://proceedings.asmedigitalcollection.asme.org/proceeding.aspx?articleid=1644765

62. Heyhat MM, Kowsary F, Rashidi AM, Alem Varzane Esfehani S, Amrollahi A. Experimental investigation of turbulent flow and convective heat transfer characteristics of alumina water nanofluids in fully developed flow regime. Int Commun Heat Mass Transf. 2012;39:1272–8.

63. Chandrasekar M, Suresh S, Chandra BA. Experimental investigations and theoretical determination of thermal conductivity and viscosity of Al_2O_3/water nanofluid. Exp Therm Fluid Sci. 2010;34:210–6.

64. Beck MP, Yuan Y, Warrier P, Teja AS. The effect of particle size on the thermal conductivity of alumina nanofluids. J Nanoparticle Res. 2009;11:1129–36.

65. Mintsa HA, Roy G, Nguyen CT, Doucet D. New temperature dependent thermal conductivity data for water-based nanofluids. International Journal of Thermal Sciences [Internet]. 2009 [cited 2018 Nov 28];48:363–71. Available from: www.elsevier.com/locate/ijts

66. Ghanbarpour M, Bitaraf Haghigi E, Khodabandeh R. Thermal properties and rheological behavior of water based Al_2O_3 nanofluid as a heat transfer fluid. Exp Therm Fluid Sci. 2014;53:227–35.

67. Patel HE, Anoop KB, Sundararajan T, Das SK. 2006, A micro-convection model for thermal conductivity of nanofluids. Nanoscale. pp 863–9

68. Li CH, Williams W, Buongiorno J, Hu L-W, Peterson GP. Transient and steady-state experimental comparison study of effective thermal conductivity of Al_2O_3/water nanofluids. J Heat Transfer. 2008;130:042407.

69. Ho CJ, Liu WK, Chang YS, Lin CC. Natural convection heat transfer of alumina-water nanofluid in vertical square enclosures: an experimental study. Int J Thermal Sci. 2010;49:1345–53.

70. Putra N, Roetzel W, Das SK. Natural convection of nano-fluids. Heat Mass Transf. 2003;39:775–84. https://doi.org/10.1007/s00231-002-0382-z.

71. Hu Y, He Y, Qi C, Jiang B, Inaki SH. Experimental and numerical study of natural convection in a square enclosure filled with nanofluid. Int J Heat Mass Transf. 2014;78:380–92. https://doi.org/10.1016/j.ijheatmasstransfer.2014.07.001.

72. Ali M, Zeitoun O, Almotairi S. Natural convection heat transfer inside vertical circular enclosure filled with water-based Al_2O_3 nanofluids. Int J Thermal Sci. 2013;63:115–24.

73. Williams W, Buongiorno J, Hu L-W. Experimental investigation of turbulent convective heat transfer and pressure loss of alumina/water and zirconia/water nanoparticle colloids (Nanofluids) in horizontal tubes. J Heat Transf. 2008;130:042412.

74. Haghighi EB, Utomo AT, Ghanbarpour M, Zavareh AIT, Poth H, Khodabandeh R, et al. Experimental study on convective heat transfer of nanofluids in turbulent flow: methods of comparison of their performance. Exp Therm Fluid Sci. 2014;57:378–87.

75. Buschmann MH. Thermal conductivity and heat transfer of ceramic nanofluids. Int J Thermal Sci. 2012;62:19–28.

76. Joshi PS, Pattamatta A. Buoyancy induced convective heat transfer in particle, tubular and flake type of nanoparticle suspensions. Int J Thermal Sci. 2017;122:1–11.

77. Ho CJ, Chang CY, Yan WM. An experimental study of forced convection effectiveness of Al_2O_3–water nanofluid flowing in circular tubes. Int Commun Heat Mass Transf. 2017;83:23–9.

78. Chougule SS, Sahu SK. Heat transfer and friction characteristics of Al_2O_3, water and CNT, water nanofluids in transition flow using helical screw tape inserts—a comparative study. Chem Eng Process: Process Intensif. 2015;88:78–88. https://doi.org/10.1016/j.cep.2014.12.005.

79. Sahin B, Gültekin GG, Manay E, Karagoz S. Experimental investigation of heat transfer and pressure drop characteristics of Al_2O_3–water nanofluid. Exp Therm Fluid Sci. 2013;50:21–8.

80. Akyürek EF, Geliş K, Şahin B, Manay E. Experimental analysis for heat transfer of nanofluid with wire coil turbulators in a concentric tube heat exchanger. Results Phys. 2018;9:376–89.

81. Hussein AM, Sharma KV, Bakar RA, Kadirgama K. The effect of nanofluid volume concentration on heat transfer and friction factor inside a horizontal tube. J Nanomater. 2013;2013:1–12.

82. Leyuan Yu, Liu D. Study of the thermal effectiveness of laminar forced convection of nanofluids for liquid cooling applications. IEEE Trans Compon Packaging Manuf Technol. 2013;3:1693–704.

83. Mathivanan E, Liu L. Impact of nanofluids on heat transfer performance of a motorcycle radiator. USA: SAE International; 2016.

84. Bin-Abdun NA, Razlan ZM, Shahriman AB, Voon CH, Wan WK, Zunaidi I, et al. The effects of nanofluid (Al2O3/

De-ionized Water) with different concentrations in improving the transportation of heat in small space. IOP Conf Ser Mater Sci Eng. 2018;429:012074. https://doi.org/10.1088/1757-899X/429/1/012074/pdf.

85. Manetti LL, Stephen MT, Beck PA, Cardoso EM. Evaluation of the heat transfer enhancement during pool boiling using low concentrations of Al_2O_3–water based nanofluid. Exp Therm Fluid Sci. 2017;87:191–200.

86. Wen D, Ding Y. Experimental investigation into the pool boiling heat transfer of aqueous based γ-alumina nanofluids. J Nanoparticle Res. 2005;7:265–74.

87. Zhu D, Wu S, Wang N. Thermal physics and critical heat flux characteristics of Al_2O_3–H_2O Nanofluids. Heat Transf Eng. 2010;31:1213–9.

88. Krzywinski M, Altman N. Visualizing samples with box plots. Nat Methods. 2014;11:119–20.

89. Scott DW. On optimal and data-based histograms. Biometrika. 1979;66:605.

90. Turian RM, Sung D-J, Hsu F-L. Thermal conductivity of granular coals, coal-water mixtures and multi-solid/liquid suspensions. Fuel. 1991;70:1157–72.

91. Keblinski P, Prasher R, Eapen J. Thermal conductance of nanofluids: is the controversy over? J Nanoparticle Res. 2008;10:1089–97. https://doi.org/10.1007/s11051-007-9352-1.

92. Bruggeman DAG. Berechnung verschiedener physikalischer Konstanten von heterogenen Substanzen. I. Dielektrizitätskonstanten und Leitfähigkeiten der Mischkörper aus isotropen Substanzen. Ann Phys. 1935;416:636–64. https://doi.org/10.1002/andp.19354160705.

93. Murshed SMS, Leong KC, Yang C. Enhanced thermal conductivity of TiO_2—water based nanofluids. Int J Thermal Sci. 2005;44:367–73.

94. Hashin Z, Shtrikman S. A variational approach to the theory of the effective magnetic permeability of multiphase materials. J Appl Phys. 1962;33:3125–31. https://doi.org/10.1063/1.1728579.

95. Jeffrey DJ. Conduction through a random suspension of spheres. Proc R Soc A: Math, Phys Eng Sci. 1973;335:355–67. https://doi.org/10.1098/rspa.1973.0130.

96. Nan C-W, Birringer R, Clarke DR, Gleiter H. Effective thermal conductivity of particulate composites with interfacial thermal resistance. J Appl Phys. 1997;81:6692–9. https://doi.org/10.1063/1.365209.

97. Hasselman DPH, Johnson LF. Effective thermal conductivity of composites with interfacial thermal barrier resistance. J Compos Mater. 1987;21:508–15. https://doi.org/10.1177/002199838702100602.

98. Xue Q, Xu W-M. A model of thermal conductivity of nanofluids with interfacial shells. Mater Chem Phys. 2005;90:298–301.

99. Yu W, Choi SUS. The role of interfacial layers in the enhanced thermal conductivity of nanofluids: a renovated maxwell model. J Nanoparticle Res. 2003;5:167–71.

100. Xie H, Fujii M, Zhang X. Effect of interfacial nanolayer on the effective thermal conductivity of nanoparticle-fluid mixture. Int J Heat Mass Transf. 2005;48:2926–32.

101. Pil Jang S, Choi SUS. Effects of various parameters on nanofluid thermal conductivity. J Heat Transfer. 2007;129:617.

102. Koo J, Kleinstreuer C. A new thermal conductivity model for nanofluids. J Nanoparticle Res. 2004;6:577–88.

103. Prasher R, Bhattacharya P, Phelan PE. Thermal conductivity of nanoscale colloidal solutions (Nanofluids). Phys Rev Lett. 2005;94:025901. https://doi.org/10.1103/PhysRevLett.94.025901.

104. Yang B. Thermal conductivity equations based on brownian motion in suspensions of nanoparticles (Nanofluids). J Heat Transfer. 2008;130:042408.

105. Ren Y, Xie H, Cai A. Effective thermal conductivity of nanofluids containing spherical nanoparticles. J Phys D Appl Phys. 2005;38:3958–61. https://doi.org/10.1088/0022-3727/38/21/019/pdf.

106. Dolatabadi N, Rahmani R, Rahnejat H, Garner CP. Thermal conductivity and molecular heat transport of nanofluids. RSC Adv. 2019;9:2516–24.

107. Murshed SMS, Leong KC, Yang C. Model for predicting the effective thermal conductivity of nanoparticle-fluid suspensions. Int J Nanosci. 2006;05:23–33. https://doi.org/10.1142/S021958 1X06004127.

108. Khodayari A, Fasano M, Bozorg Bigdeli M, Mohammadnejad S, Chiavazzo E, Asinari P. Effect of interfacial thermal resistance and nanolayer on estimates of effective thermal conductivity of nanofluids. Case Stud Thermal Eng. 2018;12:454–61.

109. Xuan Y, Li Q, Hu W. Aggregation structure and thermal conductivity of nanofluids. AIChE J. 2003;49:1038–43. https://doi.org/10.1002/aic.690490420.

110. Frost J. Regression analysis: an intuitive guide for using an interpreting linear models. UK: Life Course Research and Social Policies; 2020.

111. Zografos AI, Martin WA, Sunderland JE. Equations of properties as a function of temperature for seven fluids. Comput Methods Appl Mech Eng. 1987;61:177–87.

112. Minea AA. Uncertainties in modeling thermal conductivity of laminar forced convection heat transfer with water alumina nanofluids. Int J Heat Mass Transf. 2014;2014(68):78–84. https://doi.org/10.1016/j.ijheatmasstransfer.2013.09.018.

113. Tertsinidou G, Assael MJ, Wakeham WA. The apparent thermal conductivity of liquids containing solid particles of nanometer dimensions: a critique. Int J Thermophys. 2015;36:1367–95. https://doi.org/10.1007/s10765-015-1856-9.

114. Berger Bioucas FE, Rausch MH, Schmidt J, Bück A, Koller TM, Fröba AP. Effective thermal conductivity of nanofluids: measurement and prediction. Int J Thermophys. 2020;41:55. https://doi.org/10.1007/s10765-020-2621-2.

115. Qiu L, Zhu N, Feng Y, Michaelides EE, Żyła G, Jing D, et al. A review of recent advances in thermophysical properties at the nanoscale: from solid state to colloids. Phys Rep. 2020;843:1–81. https://doi.org/10.1016/j.physrep.2019.12.001.

116. Buonomo B, Colla L, Fedele L, Manca O, Marinelli L. A comparison of nanofluid thermal conductivity measurements by flash and hot disk techniques. J Phys Conf Ser. 2014;547:012046. https://doi.org/10.1088/1742-6596/547/1/012046.

117. Aparna Z, Michael MM, Pabi SK, Ghosh S. Diversity in thermal conductivity of aqueous Al_2O_3- and Ag-nanofluids measured by transient hot-wire and laser flash methods. Exp Therm Fluid Sci. 2018;94:231–45. https://doi.org/10.1016/j.expthermflusci.2018.02.005.

118. Xu G, Fu J, Dong B, Quan Y, Song G. A novel method to measure thermal conductivity of nanofluids. Int J Heat Mass Transf. 2019;130:978–88.

119. Eapen J, Rusconi R, Piazza R, Yip S. The classical nature of thermal conduction in nanofluids. J Heat Transfer. 2010;132:102402.

120. Li Q, Xuan Y, Wang J. Experimental investigations on transport properties of magnetic fluids. Exp Therm Fluid Sci. 2005;30:109–16.

121. Müller RH, Hildebrand GE. (1996) Zetapotential und Partikelladung in der Laborpraxis(Einführung in die Theorie praktische Messdurchführung Dateninterpretation). Wiss Verlag-Ges. 1996, 254.

122. Adegbite S. Particle characterisation and grinding behaviour of gamma-alumina slurries prepared in a stirred media mill. J Mater Sci Res. 2012;2:135.

123. Goworek J, Kierys A, Gac W, Borówka A, Kusak R. Thermal degradation of CTAB in as-synthesized MCM-41. J Therm

Anal Calorim. 2009;96:375–82. https://doi.org/10.1007/s10973-008-9055-6.

124. Jeraal MI, Roberts KJ, McRobbie I, Harbottle D. Assessment of the thermal degradation of sodium lauroyl isethionate using predictive isoconversional kinetics and a temperature-resolved analysis of evolved gases. Ind Eng Chem Res. 2019;58:8112–22. https://doi.org/10.1021/acs.iecr.9b00797.

125. Jiang W, Wang L. Copper nanofluids: synthesis and thermal conductivity. Curr Nanosci. 2010;6:512–9.

126. Evans W, Prasher R, Fish J, Meakin P, Phelan P, Keblinski P. Effect of aggregation and interfacial thermal resistance on thermal conductivity of nanocomposites and colloidal nanofluids. Int J Heat Mass Trans. 2008;51:1431–8.

127. Zhu H, Zhang C, Liu S, Tang Y, Yin Y. Effects of nanoparticle clustering and alignment on thermal conductivities of Fe_3O_4 aqueous nanofluids. Appl Phys Lett. 2006;89:023123. https://doi.org/10.1063/1.2221905.

128. Antoniadis KD, Tertsinidou GJ, Assael MJ, Wakeham WA. Necessary conditions for accurate, transient hot-wire measurements of the apparent thermal conductivity of nanofluids are seldom satisfied. Int J Thermophys. 2016;37:78. https://doi.org/10.1007/s10765-016-2083-8.

129. Hammerschmidt U, Sabuga W. Transient hot wire (THW) method: uncertainty assessment. Int J Thermophys. 2000;21:1255–78. https://doi.org/10.1023/A:1006649209044.pdf5.

130. Hasselman DPH. Can the temperature dependence of the heat transfer coefficient of the wire-nanofluid interface explain the "Anomalous" thermal conductivity of nanofluids measured by the hot-wire method? Int J Thermophys. 2018;39:109. https://doi.org/10.1007/s10765-018-2429-5.

131. Assael MJ, Wakeham WA. Comments on "Can the temperature dependence of the heat transfer coefficient of the wire-nanofluid interface explain the 'Anomalous' thermal conductivity of nanofluids measured by the hot-wire method? Int J Thermophys. 2019;40:59. https://doi.org/10.1007/s10765-019-2520-6.

132. Aybar HŞ, Sharifpur M, Azizian MR, Mehrabi M, Meyer JP. A review of thermal conductivity models for nanofluids. Heat Trans Eng. 2015;36:1085–110.

133. Eapen J, Williams WC, Buongiorno J, Hu L, Yip S, Rusconi R, et al. Mean-field versus microconvection effects in nanofluid thermal conduction. Phys Rev Lett. 2007;99:095901. https://doi.org/10.1103/PhysRevLett.99.095901.

134. Azizian MR, Aybar HŞ, Okutucu T (2009) Effect of nanoconvection due to Brownian motion on thermal conductivity of nanofluids. In: Proceedings of the 7th IASME/WSEAS international conference on heat transfer, Thermal Engineering and Environment, HTE '09. pp 53–6

135. Pang C, Lee JW, Kang YT. Enhanced thermal conductivity of nanofluids by nanoconvection and percolation network. Heat Mass Transf. 2016;52:511–20.

136. Azizian R, Doroodchi E, Moghtaderi B. Effect of nanoconvection caused by brownian motion on the enhancement of thermal conductivity in nanofluids. Ind Eng Chem Res. 2012;51:1782–9. https://doi.org/10.1021/ie201110k.

137. Cardellini A, Fasano M, Bozorg Bigdeli M, Chiavazzo E, Asinari P. Thermal transport phenomena in nanoparticle suspensions. J Phys: Condens Matter. 2016;28:483003.

138. Piazza R, Parola A. Thermophoresis in colloidal suspensions. J Phys: Condens Matter. 2008;20:153102.

139. Liu C, Fang H, Qiao Y, Zhao J, Rao Z. Properties and heat transfer mechanistic study of glycerol/choline chloride deep eutectic solvents based nanofluids. Int J Heat Mass Transf. 2019;138:690–8.

140. Turanov AN, Tolmachev YV. Heat- and mass-transport in aqueous silica nanofluids. Heat Mass Transf. 2009;45:1583–8. https://doi.org/10.1007/s00231-009-0533-6.

141. Gerardi C, Cory D, Buongiorno J, Hu L-W, McKrell T. Nuclear magnetic resonance-based study of ordered layering on the surface of alumina nanoparticles in water. Appl Phys Lett. 2009;95:253104. https://doi.org/10.1063/1.3276551.

142. Ge Z, Cahill DG, Braun PV. Thermal conductance of hydrophilic and hydrophobic interfaces. Phys Rev Lett. 2006;96:186101. https://doi.org/10.1103/PhysRevLett.96.186101.

143. Milanese M, Iacobazzi F, Colangelo G, de Risi A. An investigation of layering phenomenon at the liquid–solid interface in Cu and CuO based nanofluids. Int J Heat Mass Transf. 2016;103:564–71.

144. Muraleedharan MG, Sundaram DS, Henry A, Yang V. Thermal conductivity calculation of nano-suspensions using Green-Kubo relations with reduced artificial correlations. J Phys Condens Matter. 2017;29:155302.

145. Liang Z, Tsai H-L. Thermal conductivity of interfacial layers in nanofluids. Phys Rev E. 2011;83:041602. https://doi.org/10.1103/PhysRevE.83.041602.

146. Dong R-Y, Zhou Y, Yang C, Cao B-Y. Experimental study on thermophoresis of colloids in aqueous surfactant solutions. J Phys Cond Matter. 2015;27:495102.

147. Piazza R. Thermophoresis: moving particles with thermal gradients. Soft Matter. 2008;4:1740.

148. Michaelides EE. Brownian movement and thermophoresis of nanoparticles in liquids. Int J Heat Mass Transf. 2015;81:179–87.

149. Ho CJ, Chen D-S, Yan W-M, Mahian O. Buoyancy-driven flow of nanofluids in a cavity considering the Ludwig-Soret effect and sedimentation: numerical study and experimental validation. Int J Heat Mass Transf. 2014;77:684–94.

150. Sergis A, Hardalupas Y. Revealing the complex conduction heat transfer mechanism of nanofluids. Nanoscale Res Lett. 2015;10:250. https://doi.org/10.1186/s11671-015-0954-8.

151. Berg JC. An introduction to interfaces and colloids. India: World Scientific; 2009.

152. Yu F, Chen Y, Liang X, Xu J, Lee C, Liang Q, et al. Dispersion stability of thermal nanofluids. Progress Nat Sci Mater Int. 2017;27:531–42.